



ELSEVIER

Journal of Volcanology and Geothermal Research 113 (2002) 81–110

Journal of volcanology
and geothermal research

www.elsevier.com/locate/jvolgeores

Debris avalanches and debris flows transformed from collapses in the Trans-Mexican Volcanic Belt, Mexico – behavior, and implications for hazard assessment

L. Capra^{a,*}, J.L. Macías^b, K.M. Scott^c, M. Abrams^d,
V.H. Garduño-Monroy^e

^a Instituto de Geografía, UNAM, Coyoacán 04510, Mexico D.F., Mexico

^b Instituto de Geofísica, UNAM, Mexico D.F., Mexico

^c Cascades Volcano Observatory, Vancouver, WA, USA

^d Jet Propulsion Laboratory, California Institute of Technology, Pasadena, CA, USA

^e Universidad Michoacana de San Nicolás de Hidalgo, Morelia, Mexico

Received 19 March 2001; received in revised form 14 June 2001; accepted 14 June 2001

Abstract

Volcanoes of the Trans-Mexican Volcanic Belt (TMVB) have yielded numerous sector and flank collapses during Pleistocene and Holocene times. Sector collapses associated with magmatic activity have yielded debris avalanches with generally limited runout extent (e.g. Popocatepetl, Jocotitlán, and Colima volcanoes). In contrast, flank collapses (smaller failures not involving the volcano summit), both associated and unassociated with magmatic activity and correlating with intense hydrothermal alteration in ice-capped volcanoes, commonly have yielded highly mobile cohesive debris flows (e.g. Pico de Orizaba and Nevado de Toluca volcanoes). Collapse orientation in the TMVB is preferentially to the south and northeast, probably reflecting the tectonic regime of active E–W and NNW faults. The differing mobilities of the flows transformed from collapses have important implications for hazard assessment. Both sector and flank collapse can yield highly mobile debris flows, but this transformation is more common in the cases of the smaller failures. High mobility is related to factors such as water content and clay content of the failed material, the paleotopography, and the extent of entrainment of sediment during flow (bulking). The ratio of fall height to runout distance commonly used for hazard zonation of debris avalanches is not valid for debris flows, which are more effectively modeled with the relation inundated area to failure or flow volume coupled with the topography of the inundated area. © 2002 Elsevier Science B.V. All rights reserved.

Keywords: Trans-Mexican Volcanic Belt; debris avalanche; cohesive debris flow; hazard assessment

1. Introduction

The occurrence of the 1980 sector collapse and debris avalanche at Mount St. Helens triggered the recognition of uniquely hummocky deposits of many analogous debris avalanches at volcanoes

* Corresponding author. Tel.: +52-5-6224124;
fax: +52-5-5502486.

E-mail address: solari@servidor.unam.mx (L. Capra).

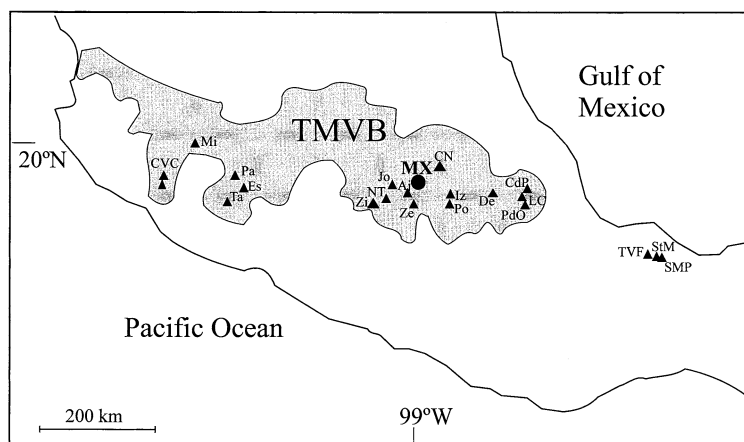


Fig. 1. Sketch map of the TMVB showing the location of the volcanoes with known sector collapse: Colima Volcanic Complex (CVC), Milpilla (Mi), Patamban (Pa), Estribo (Es), Tancitaro (Ta); Zirahuato (Zi), Jocotitlán (Jo), Nevado de Toluca (NT), Zempoala (Ze), Ajusco (Aj), Iztaccihuatl (Iz), Popocatepetl (Po), Cerro Las Navajas (CN), Las Derrumbadas (De), Pico de Orizaba (PdO), Las Cumbres (LC), and Cofre de Perote (CdP). Santa Martha (StM), San Martín Pajapan (SMP) and Los Tuxtlas Volcanic Field (TVF) not in the TMVB are also shown.

worldwide (Siebert, 1984; Ui et al., 1986; Siebert et al., 1987; Vallance et al., 1995; Francis and Wells, 1988). Subsequent studies revealed the occurrence of edifice collapses and the flows transformed from them at several of the better-known volcanoes of the Trans-Mexican Volcanic Belt (TMVB) (Fig. 1): Nevado de Colima and Volcán de Fuego volcanoes (Robin et al., 1987, 1990; Luhr and Prestegard, 1988; Stoope and Sheridan, 1992; Komorowski et al., 1994, 1997), Jocotitlán v. (Siebe et al., 1992, 1995a), Nevado de Toluca v. (Macías et al., 1997; Capra and Macías, 2000), Popocatepetl v. (Robin and Boudal, 1987; Siebe et al., 1995b; Lozano-Velazquez and Carrasco-Núñez, 1997), Las Derrumbadas (Siebe et al., 1995a) and Pico de Orizaba (Carrasco-Núñez and Gomez-Tuena, 1997; Carrasco-Núñez et al., 1993; Hoskuldsson and Robin, 1993). Debris avalanche and debris flow deposits of probable similar origin are known from the stratigraphic record at many other Mexican volcanoes but remain to be described in detail. The magnitude and frequency that can be inferred from the known deposits (Table 1) clearly indicate that flows of this origin are a significant volcanic hazard in the TMVB.

The aim of this paper is to present a bibliography of the occurrences of debris avalanche depos-

its and other kind of flows transformed from volcano collapses in Mexico and to analyze the hazard implications of these occurrences. We described each case history based on the available bibliography, by stratigraphy, textural characteristics, the dimensions of the deposits (runout distance, area, and volume), and on what is known about the source area.

In addition, Landsat Thematic Mapper (TM bands 3, 4 and 7) images have been elaborated to provide further information about the distribution and the morphological characteristics of the debris avalanche deposits described in the text.

2. Terminology

A debris avalanche is a rapidly moving incoherent and unsorted mass of rock and soil mobilized by gravity (Schuster and Crandell, 1984). The terminology proposed by Glicken (1991) is used here to describe the deposits deriving from it. Two end-member facies define deposit texture: block facies and mixed (matrix) facies. The block facies is composed mainly of debris avalanche blocks (an unconsolidated piece of the old mountain transported to its place of deposition) with practically no matrix. The mixed facies is a mixture of

Table 1
Location and characteristics of the known cases of debris avalanche deposits in Mexico

Name (acronym)	Latitude, longitude	Elevation (m asl)	Type of collapse-related activity	Type of deposit	<i>D</i>	<i>A</i> (km ²)	<i>L</i> (km)	<i>V</i> (km ³)	<i>H/L</i>	Age	Ref.
Nevado de Colima (NC)	19°33'48"N, 103°36'30"W	4240	Bezymianny-type	Block and matrix facies DAD, average thickness of 15 m, monolithologic with andesitic lava fragments.	E	2200	120	22–33	0.04	18 520 ± 260 yr BP	1, 2
Volcan de Colima (VC)	19°30'40"N, 103°37'W	3820	Bezymianny-type	Block and matrix facies DAD, mean thickness of 10 m, monolithologic with andesite lava fragments.	SW	1200	43	6–12	0.09	9 370 ± 400 yr BP 4 280 ± 110 yr BP	2 3
Nevado de Toluca (NT)	19°09'N, 99°45'W	4565	Non-volcanic (water-saturated, hydrothermally altered volcano)	<i>Pilcaya deposit</i> . Matrix-supported cohesive DFD, average thickness of 20 m, heterolithologic with clasts of basalt, dacite and secondary fragments from bedrock.	S	100	55	2	0.054	Pleistocene	4, 5
Nevado de Toluca (NT)	19°09'N, 99°45'W	4565	Non-volcanic (water-saturated, hydrothermally altered volcano)	<i>Mogote deposit</i> . Matrix-supported cohesive DFD, average thickness of 10 m, heterolithologic with clasts of basalt, dacite and secondary fragments from bedrock.	S	120	75	0.8	nd	Pleistocene	4, 5
Jocotitlán (Jo)	19°43'25"N, 99°45'25"W	3950	Bezymianny-type	Block facies DAD, with hummocks up to 185 m high, monolithologic with dacitic lava fragments.	NE	80	12	2.8	0.11	9 690 ± 89 yr BP	6
Zempoala (Ze)	19°03'N, 99°20'W	3800	Non-volcanic (water-saturated, hydrothermally altered volcano)	Matrix-supported DFD, average thickness of 10 m, heterolithologic with clasts of basalt, dacite and secondary fragments from bedrock.	S	400	80	4	0.04	Pliocene	5
Popocatepetl (Po)	19°03'N, 98°35'W	5452	Bezymianny-type	Block and matrix facies DAD, average thickness of 15 m, heterolithologic with clasts of andesite and dacite and fragments of older pyroclastic deposits.	S	600	70	9	0.064	22 875 ± 915/ –820 yr BP	7, 8

Table 1. (continued)

Name (acronym)	Latitude, longitude	Elevation (m asl)	Type of collapse-related activity	Type of deposit	<i>D</i>	<i>A</i> (km ²)	<i>L</i> (km)	<i>V</i> (km ³)	<i>H/L</i>	Age	Ref.
Iztaccihuatl (Iz)	19°10'N, 98°38'W	5285	nd	nd	SW	50	nd	0.5	nd	nd	7
Pico de Orizaba (PdO)	19°02'N, 97°17'W	5675	nd	<i>Jamapa deposit.</i> Block and mixed facies DAD, average thickness of 50 m, heterolithologic in composition.	ENE	350	95	20	nd	Pleistocene	9, 10
Pico de Orizaba (PdO)	19°02'N, 97°17'W	5675	Non-volcanic (water-saturated, hydrothermally altered volcano)	<i>Tetelzingo deposit.</i> Matrix-supported cohesive DFD, with mean thickness of 12 m, heterolithologic in composition with clasts of andesite and dacite.	ENE	143	85	1.8	0.055	27 000–13 000 yr BP	9, 10
Las Derrumbadas (De)	19°18'N, 97°28'W	4240	Dome growth	<i>First generation deposit.</i> Block and mixed facies DAD, heterolithologic composed of obsidian, fragments of pyroclastic deposits, and rocks from the bedrock.	nd	nd	9	nd	0.1	nd	11
Las Derrumbadas (De)	19°18'N, 97°28'W	4240	Dome instability (hydrothermally altered portions of domes)	<i>Second generation deposits.</i> Mixed facies DAD, monolithologic in composition with rhyolitic clasts.	nd	nd	4.5	nd	0.2	nd	11
Cofre de Perote (CdP)	19°30'N, 97°10'W	4282	nd	nd	ESE	nd	nd	nd	nd	<0.24 ± 0.05 Ma	12
Las Cumbres (LC)	19°10'N, 97°15'W	3940	nd	Mixed facies DAD, monolithologic in composition with rhyolitic clasts.	E	nd	nd	nd	nd	40 000 yr BP	13
Cerro Las Navajas (CN)	20°12'N, 98°33'W	3180	nd	Block and mixed facies DAD, up to 100 m thick, heterolithologic in composition with clasts of rhyolite, basalt and fragments of older pyroclastics sequences.	NW	560	nd	35 ± 10	nd	> 1.8 Ma	14
Ajusco (Aj)	19°13'N, 99°15'W	3906	Bandai-type	Block and mixed facies DAD, heterolithologic in composition with clasts of andesite and dacite.	NE	nd	16	1.7	nd	nd	15

Table 1. (continued)

Name (acronym)	Latitude, longitude	Elevation (m asl)	Type of collapse-related activity	Type of deposit	<i>D</i>	<i>A</i> (km ²)	<i>L</i> (km)	<i>V</i> (km ³)	<i>H/L</i>	Age	Ref.
Tancítaro (Ta)	19°22'N, 102°21'W	3600	Non-volcanic (water-saturated, hydrothermally altered volcano)	Matrix-supported DFD, average thickness of 20 m, heterolithic in composition with clasts of andesite and dacite.	NE	176	60	3.52	nd	< 10 000 yr BP	16
Patamban (Pa)	19°45'N, 102°20'W	3400	Bezymianny-type(?)	Block and mixed DAD, average thickness of 10 m, monolithic in composition with andesitic clasts.	SW	25	9	0.25	nd	nd	16
Zirahuato (Zi)	19°31'30"N, 100°32'W	2750	Bezymianny-type(?)	Block and mixed DAD, average thickness of 10 m, monolithic in composition with dacitic clasts.	SW	1.5	2	0.07	nd	50 000 yr BP	16, 17
Milpilla (Mi)	20°09'N, 103°23'W	2150	Non-volcanic (tectonic-induced)	nd	SW	4	3.5	0.07	nd	< 5 000 yr BP?	16
Estribo (Es)	19°30'45"N, 101°38'30"W	2500	Non-volcanic (tectonic-induced)	Block facies DAD, average thickness of 50 m, monolithic in composition with andesitic clasts.	N	4	9	0.2	nd	< 45 000 yr BP	16
San Martín Pajapan (SMP)	18°16'N, 95°44'W	1250	nd	nd	S	nd	nd	nd	nd	nd	5
Santa Martha (StM)	18°20'N, 95°35'W	1000	nd	Mixed facies DAD, average thickness of 15 m, heterolithic in composition with clasts of basalt and andesite.	NE	73	20	1	nd	< 1 Ma	5

DAD: debris avalanche deposit; DFD: debris flow deposit; *D*: collapse direction; *A*: area; *L*: maximum runout distance; *V*: volume; nd: not determined.

References: 1: Stoope and Sheridan (1992); 2: Robin et al. (1987); 3: Luhr and Prestegard, 1988; 4: Capra and Macías (2000); 5: this work; 6: Siebe et al. (1992); 7: Siebe et al. (1995b); 8: Robin and Boudal (1987); 9: Carrasco-Núñez et al. (1993); 10: Hoskuldsson and Robin (1993); 11: Siebe et al. (1995a); 12: Lozano-Velázquez and Carrasco-Núñez (2000); 13: Rodríguez-Elizarrarás and Komorowski, 1997; 14: Nelson and Lighthart, 1997; 15: Cervantes et al. (1994); 16: Garduño-Monroy et al., 1999; 17: Demant (1978).

clasts and interclast matrix and may contain clasts of all rock types and of sizes from micrometers to meters.

In proximal areas the surface of volcanic debris avalanche deposits generally consists of mounds (hummocks or cerrillos) consisting of single debris avalanche blocks; in distal areas the surfaces are generally flat, with fewer mounds but with lateral levees and, in the cases of flows that did not transform to debris flows, an abrupt front. Mounds are the most distinguishing characteristic of volcanic debris avalanches and are the primary basis for recognition of several hundred large deposits of the flows around the world.

Debris flow defines a flowing mixture of debris and water having sediment concentration between 70% and 90% by weight (Pierson and Costa, 1987). When the clay fraction is $> 3\%$ in weight of the matrix (sand+silt+clay), they are defined as cohesive debris flows (Scott et al., 1995). This relatively clay-rich texture commonly defines debris flows originating as volcanic collapses or landslides, with the clay formed by hydrothermal alteration within the edifice. Cohesive debris flows contrast with noncohesive flows which originate as meltwater surges during eruptions, yielding granular, relatively clay-poor deposits. Cohesive debris flow deposits are commonly matrix-supported, massive, graded, and commonly exhibit a distinct trend in sedimentological characteristics, such as improvement of sorting with distance and decrease or increase of the mean grain size values depending on the processes acting during flow transport. In contrast, debris avalanche deposits generally have less significant variations in sedimentological parameters with distance. This difference reflects the different mechanisms of transport and emplacement for these two types of flows.

Lahar is a general term for a volcanic debris flow or, more generally, any rapidly flowing water-saturated mixture of rock debris and water from a volcano (Smith and Fritz, 1989). This definition considers a lahar as an event and does not refer to the deposit produced by it, as also pointed out by Vallance (2000) who defines lahar as a process for the formation of a debris flow, transitional flow or hyperconcentrated flow from

a volcano. Here, we use the term lahar only to specify the origin of the flow, as in the case of a deposit originating from the remobilization of unconsolidated volcanic material.

Sector collapses are large volcanic landslides that remove the summit of the failed volcano, leave an open, horseshoe-shaped crater, and generally have a volume in excess of 1 km^3 , in cases as much as several tens of km^3 . We distinguish as flank collapses the smaller failures that do not include the volcano summit.

3. Origin of edifice instability and triggering mechanisms

The instability of a volcanic edifice is promoted by many factors directly related to volcanic activity as well as exogenous processes such as weathering. These factors include direct magmatic intrusion into the edifice (Bezymianny-type activity, Gorshkov, 1962) or subvolcanic crust (Elsworth and Voight, 1996; Day, 1966), deposition of voluminous pyroclastic deposits on steep slopes (McGuire, 1996), hydromagmatic processes (Dzurisin, 1998), and phreatomagmatic activity (Bandai-type activity, Moriya, 1980).

Progressive weakening of a volcanic edifice by hydrothermal alteration is the fundamental indirect factor leading to collapse (Frank, 1983; Carrasco-Núñez et al., 1993; Vallance and Scott, 1997). Cohesive debris flows mobilize directly from flank collapses of saturated, highly altered and clay-rich material (Scott et al., 1995, 2001; Crowley and Zimbelman, 1997; Vallance and Scott, 1997). This direct transformation from a debris avalanche to a cohesive debris flow may be associated with: (1) failure within a soil, rock, or sediment mass; (2) partial or complete liquefaction of the mass by high pore-fluid pressures; and (3) conversion of landslide translational energy to internal vibrational energy (see Iverson, 1997, for a summary of failure mechanics). In addition, cohesive debris flow can also originate in other ways, such as: (1) transformation during transport of the distal portion of a water-saturated debris avalanche (Palmer and Neall, 1989); (2) post-depositional remobilization

of water-saturated portions of a debris avalanche (Glicken, 1998); and (3) rupture of natural dams originating as debris avalanches (Costa, 1988; Costa and Schuster, 1988).

The tectonic setting of the volcano may influence the direction of collapse (Siebert, 1984), and in some cases faulting may trigger collapse (McGuire, 1996). In addition, the mass of the volcano can induce isostatic flexure, compaction, and deformation that can lead directly to collapse (Borgia et al., 1992; van Wyk de Vries and Borgia, 1996).

Although simple gravitational failure may occur in response to progressive weakening of an edifice, discrete triggering mechanisms are commonly independent of the processes producing edifice instability. Keefer (1984) established that numerous large landslides during historic time were triggered by earthquakes. Schuster and Crandell (1984) determined that approximately 35% of landslides causing natural dams were seismogenic. The most recent example of a catastrophic seismogenic flow from volcanic terrain occurred in 1994 in Colombia in response to a tectonic earthquake of 6.4 M (Scott et al., 2001). Saturated by recent rainfall (Avila et al., 1995; INGEOMINAS, 1995), more than 3000 shallow failures coalesced with flank collapses of Nevado del Huila volcano to produce a single wave of cohesive debris flow that traveled over 100 km and caused as many as 1000 fatalities. Other triggering mechanisms include phreatic explosions and precipita-

Table 2

^{14}C radiocarbon ages (yr BP) obtained from paleosol layers interbedded with debris avalanche deposits (after Komorowski et al., 1997)

Volcán de Colima	Nevado de Colima
2 565	
3 699	
7 000	
9 700	
14 885	
18 240	18 553
21 500	
27 800	
35 780	
39 092	
45 030	

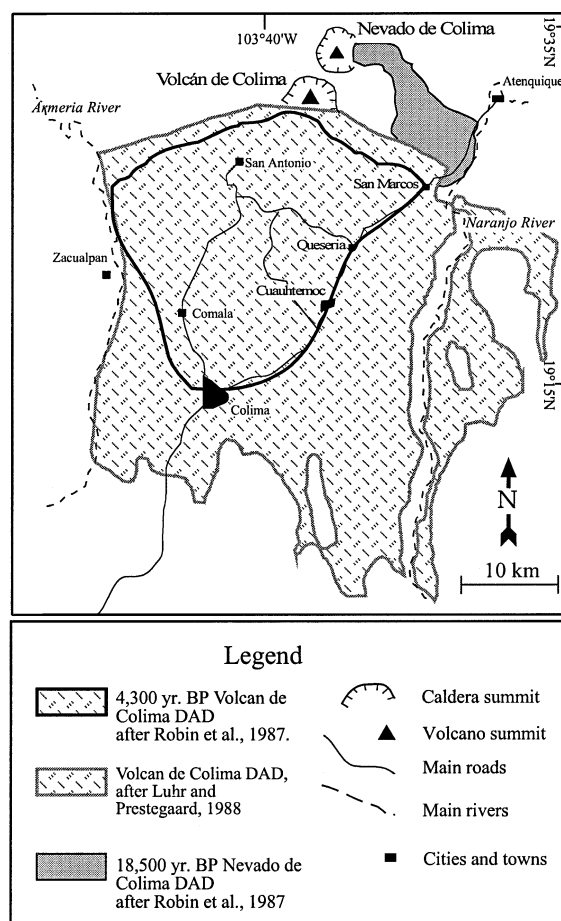


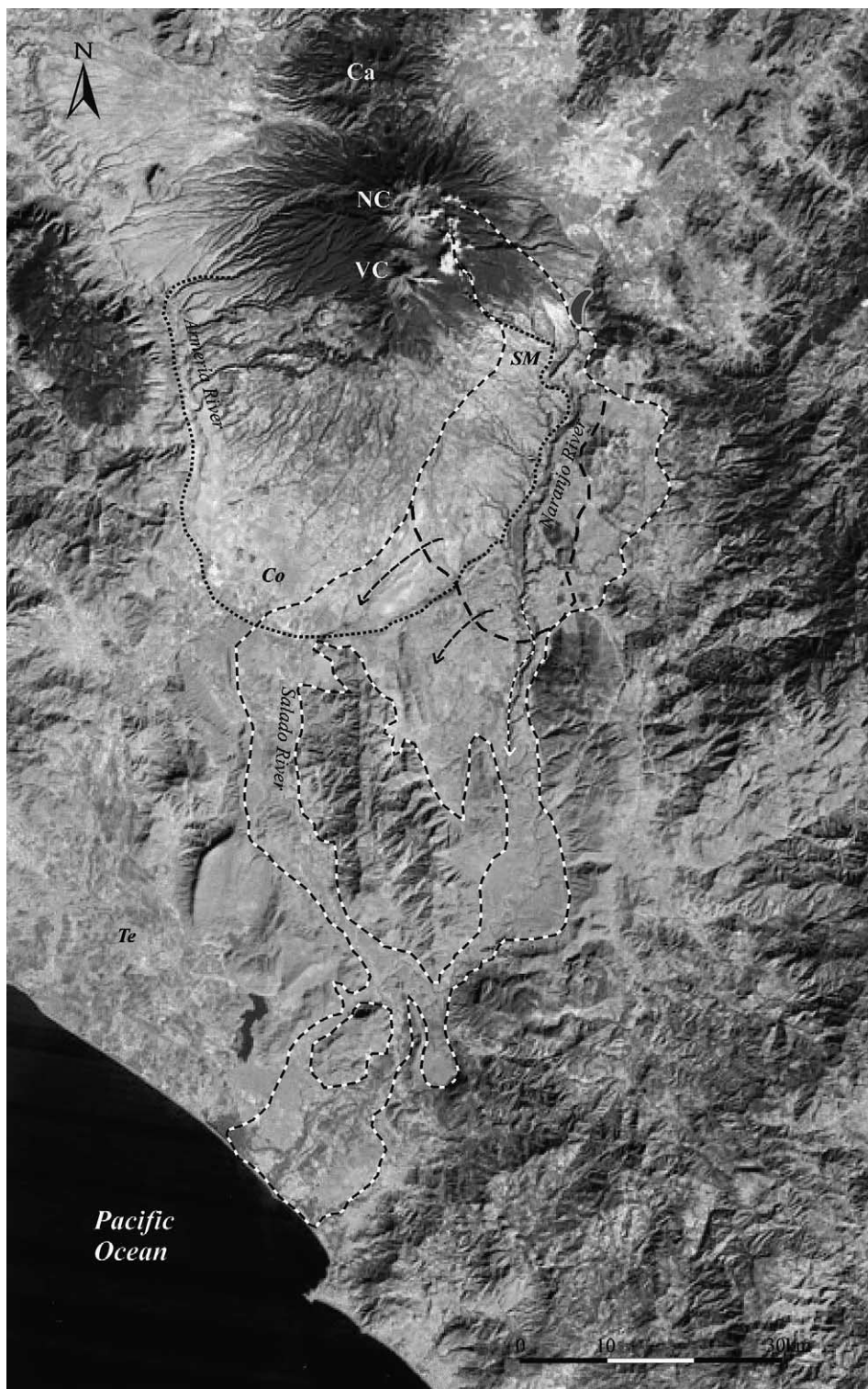
Fig. 2. Distribution of the debris avalanche deposits at the CVC (after Robin et al., 1987; Luhr and Prestegard, 1988).

tion. Hurricane-induced rainfall triggered flank collapse at Casita volcano in Nicaragua in 1998 that killed 2500 people (Sheridan et al., 1999; Scott et al., 2002).

4. The Colima Volcanic Complex

The Colima Volcanic Complex (CVC, Figs. 1–3, Table 1) is located at the western end of the TMVB, at the southern limit of the Colima Graben. It consists of three andesitic composite cones, Cántaro, Nevado de Colima and Volcán de Colima.

Nevado de Colima volcano (4240 m asl) has an



approximate age of ca. 600 000 years. A paleosol overlying a pyroclastic flow deposit yields an age of 8100 radiocarbon years (Robin et al., 1990), a limiting minimum age for volcanic activity at this cone. No younger deposits are known. Three main episodes characterized this edifice (Nevado I, II and III; Robin et al., 1987). During the Nevado II period a sector collapse yielded a debris avalanche deposit, probably associated with an east-facing horseshoe-shaped crater, 4 km in width (Robin et al., 1987; Stoopes and Sheridan, 1992). Stoopes and Sheridan (1992) determined the age of this deposit as $18\,520 \pm 260$ yr BP, based on a carbonized tree found in the deposit.

Volcán de Colima (3820 m asl) is the active composite cone, with a maximum age of about 50 000 years (Robin et al., 1987). Major eruptions occurred in 1913, 1981, 1991 and 1998–99/2000. Paleofuego is the older part of the edifice, which consists of a south-facing horseshoe-shaped crater on which the active cone has been constructed. Luhr and Presteggaard (1988) described a debris avalanche deposit exposed south of the edifice with an age of 4280 ± 110 yr BP, contrasting with an age reported by Robin et al. (1987) of 9370 ± 400 yr BP for the same deposit. The age reported by Luhr and Presteggaard (1988) was obtained from charcoal found in a pyroclastic surge deposit directly overlying the debris avalanche deposit, while the age reported by Robin et al. (1987) was obtained from a charcoal found on a pyroclastic flow deposit below the avalanche unit. These two ages are contrasting and they likely represent the maximum and minimum ages of the deposit.

Komorowski et al. (1997) presented a different scenario for both volcanoes, proposing that collapse has occurred at least 12 times in the last 45 000 years and perhaps as many as nine times

from the younger edifice. Their hypothesis is based on radiocarbon ages of paleosols and lacustrine deposits interbedded with debris flow units interpreted as debris avalanche deposits. Table 2 presents the radiocarbon ages related to those collapse events. Because of the unknown extent of these deposits, we do not present correlations between individual units.

Robin et al. (1987) described the ~ 18 ka BP debris avalanche deposit at Nevado de Colima volcano as a Bezymianny-type event. They determined that the flow extended up to 20 km southeast of the edifice, transforming to lahars between the towns of San Marcos and Atenquique (Fig. 2). Stoopes and Sheridan (1992) believed that the flow traveled up to 120 km from the summit, covering an area of 2200 km² with a total volume of 22–33 km³ (Fig. 3). The deposit exhibits hummocky morphology to within 3 km of the coastline, with individual mounds up to 10 m high. The deposit consists of both block and matrix facies, with andesite blocks and juvenile andesite blocks with bread-crust texture. In some outcrops a tephra layer lies directly on the avalanche deposit (Stoopes and Sheridan, 1992). Stoopes and Sheridan (1992) measured an *H/L* of 0.04 and applied energy-line concepts (Hsu, 1975) to calculate average velocities of 78 m/s at 42 km and 44 m/s at 90 km from the volcano. These authors ascribed the high mobility of the flow as reflecting a magmatic component with a large amount of gases and hydrothermal fluids. The topography of the runout area is another factor that may have facilitated speed and mobility. Although Robin et al. (1987, 1990) and Stoopes and Sheridan (1992) considered the huge deposit to have come from collapse of Nevado de Colima volcano, Capra and Macías (1999, 2002) concluded that the first 30 km of the deposit was a debris avalanche, but

Fig. 3. Landsat image of the CVC showing the distribution of the Nevado de Colima (NC) (black-and-white dashed line) and Volcán de Colima (VC) (black dotted line) debris avalanche deposits after Stoopes and Sheridan (1992). The black dashed line indicates the southern limit of the debris avalanche deposit according to Capra and Macías (2002). According to these authors the deposit formed a temporary dam (white closed line) which ruptured forming a 10-km³ break-out debris flow deposit along the Naranjo River (black-and-white arrow indicates the flow direction). Secondary lahars also formed from the dewatering of the debris avalanche itself (black arrows). The Cántaro Volcano (Ca) is the oldest volcanic center of the CVC. Main towns are Colima (Co), San Marcos (SM) and Tecomán (Te).

from the Naranjo River outcrops to the Pacific coast (more than 90 km) the deposit was a debris flow derived from secondary remobilization of the debris avalanche (Fig. 3). Texture and sedimentology of the deposit along the Naranjo River suggest that this unit represents a cohesive debris flow deposit derived from a water-saturated debris avalanche after that flow was emplaced. Evi-

dence includes the massive structure, a matrix-supported texture, the longitudinal variation of the sedimentological parameters (improving of mean grain size and sorting), and imbrication of secondary clasts bulked into the flow during its transport (Capra and Macías, 2002). In addition, the debris flow deposit contains clasts with typical jigsaw puzzle texture, characteristic of a debris

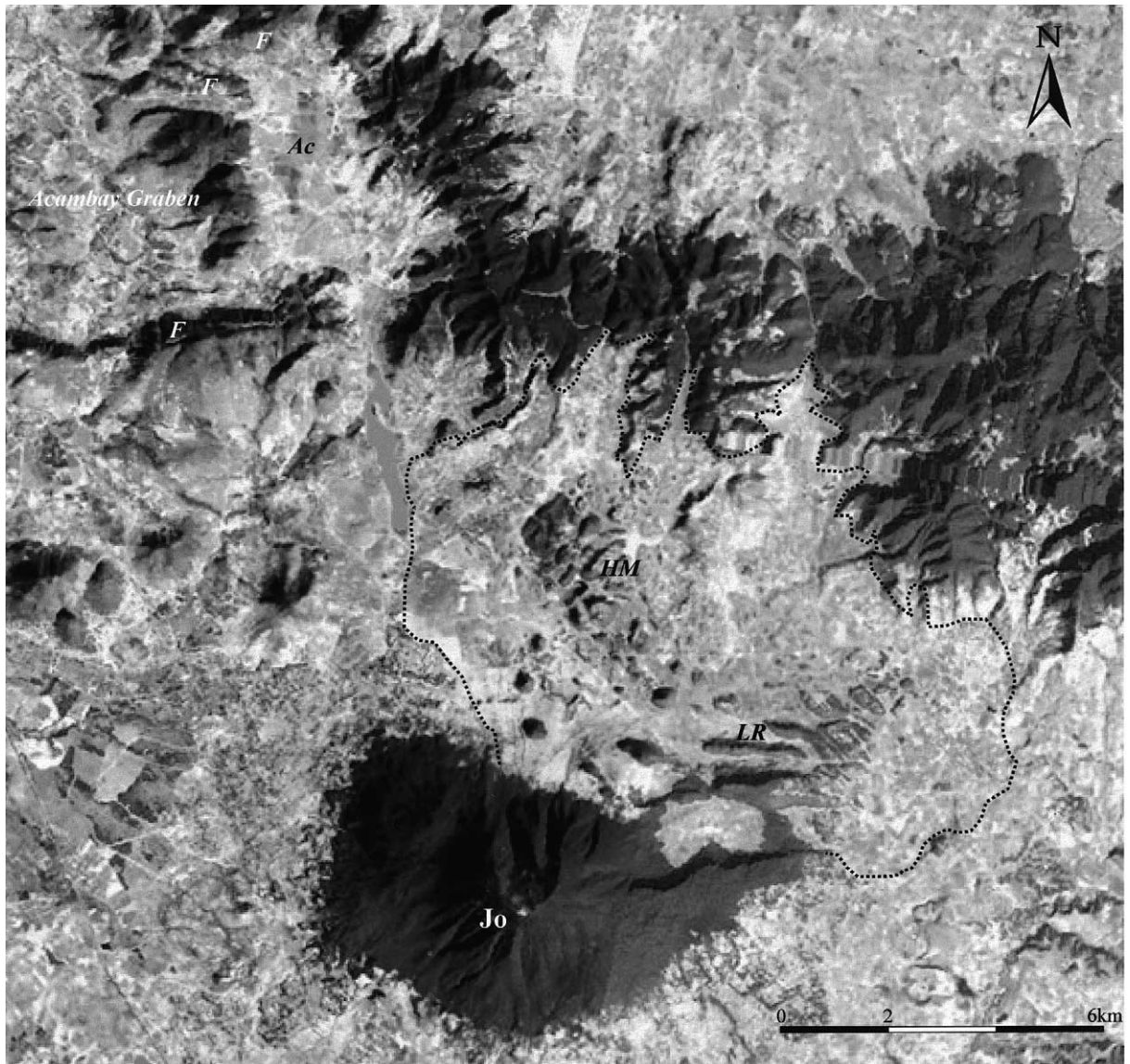


Fig. 4. Landsat image of the Jocotitán volcano (Jo). The black dotted line indicates the limit of the debris avalanche deposit which is characterized by a well defined hummocky morphology (HM) and lateral ridges (LR) (after Siebe et al., 1992). The main town is Acambay (Ac) located within the Acambay Graben (F: fault which limits the graben).

avalanche deposit. Capra and Macías (2002) proposed that the collapse formed a debris avalanche deposit which had a volume of 7 km³ and extended up to a distance of 45 km. The debris avalanche then stopped against a topographic barrier (Cerro La Carbonera), temporarily damming the Naranjo River (Fig. 3). The superficial remobilization of the debris avalanche deposit first formed a secondary lahar that inundated the southern plain and entered the Salado River drainage. Subsequently, the blockage on the Naranjo River may have failed and become remobilized as a series of debris flows which possibly coalesced to create a catastrophic flow that reached the Pacific coast more than 90 km from the volcano with a volume of 10 km³ (Capra and Macías, 2002). If we estimate that approximately 1.5 km³ of the debris avalanche deposit was remobilized, the downstream debris flow increased in volume up to six times due to bulking of material from the basement and from the river bed.

A ~4000 yr BP debris avalanche deposit extends from the Volcán de Colima edifice to a distance of 70 km, covering an area of 1550 km² with a volume of 10 km³ and an H/L of 0.06 (Fig. 2). Stoores and Sheridan (1992) and Robin et al. (1987) obtained lower figures for those parameters, and they also calculated a higher H/L , 0.09 (Figs. 2 and 3). The deposit is composed of an unsorted, unstratified mix of angular, brecciated andesite clasts, with small (0.5–1.0 m) debris avalanche blocks of the same lithology. In contrast to the interpretation of these deposits as those of numerous primary, untransformed debris avalanches (Komorowski et al., 1997), our field reconnaissance suggests that many of them correspond to debris flow units that may have originated from dewatering of debris avalanche deposits after their emplacement, or as lahars formed after failures of river blockages as occurred at the Nevado de Colima volcano during the 18 500 yr BP collapse event.

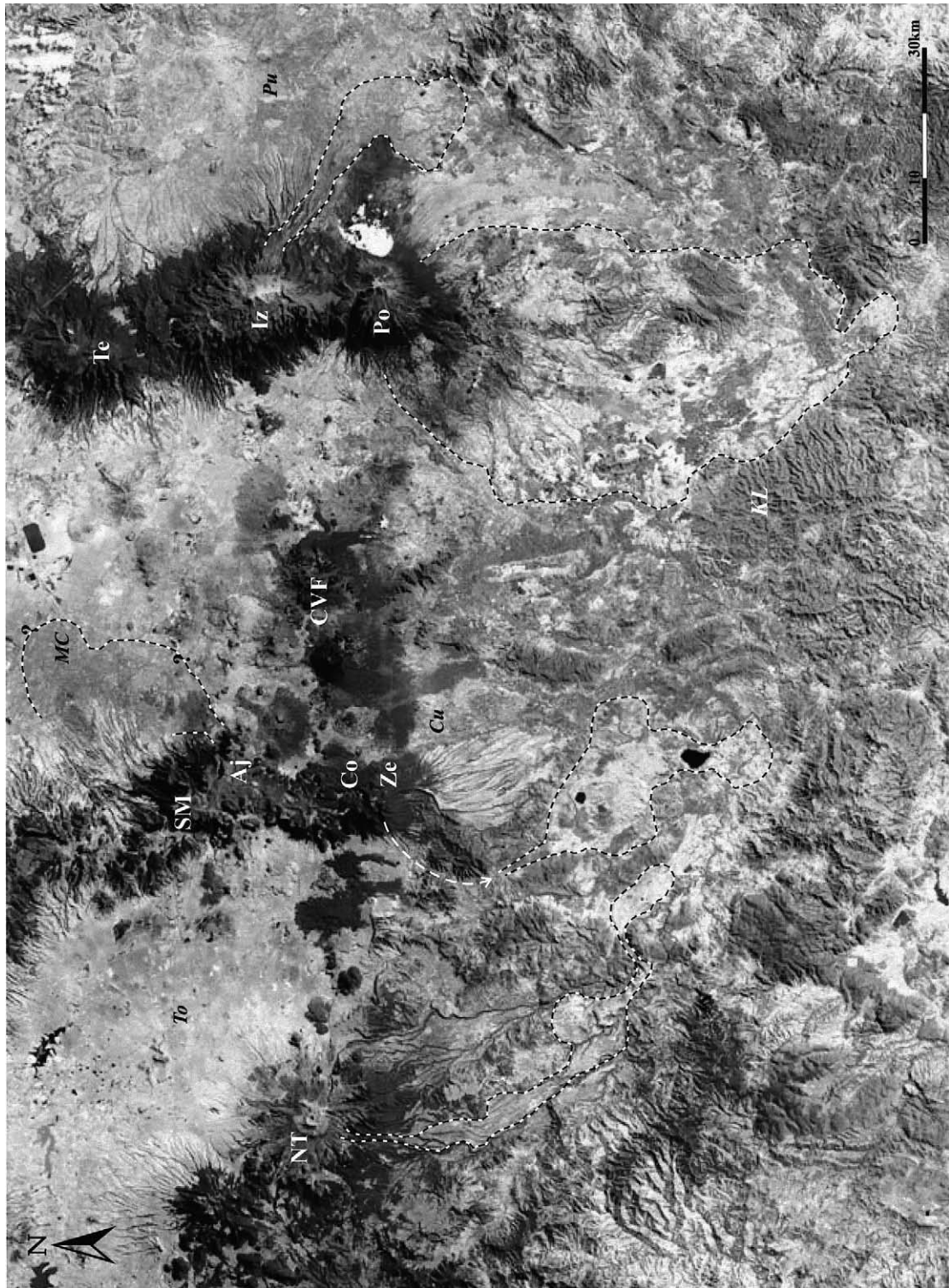
The relation of collapses to eruptive activity at the CVC has not been studied in detail. However, Robin et al. (1990) described pyroclastic surge deposits directly associated with the debris avalanche deposits at Volcán de Colima and Nevado de Colima volcanoes which show a bimodal com-

position of the juvenile material. From this observation, they concluded that the collapse events may relate to major changes in the petrologic evolution of the volcanoes, with the injection of a mafic magma in a stratified andesitic or dacitic magma chamber, followed by the start of a new magmatic cycle.

5. The Jocotitlán volcano

The Jocotitlán volcano (Jo, Figs. 1 and 4, Table 1) is a dacitic composite cone, with the most recent activity dated as 680 radiocarbon years by Siebe et al. (1992). A horseshoe-shaped crater faces NE, clearly associated with the debris avalanche deposit at the base of the edifice (Fig. 4). This unit covers an area of 80 km², has a maximum runout distance L of 12 km, and a maximum fall height H of 1150 m, corresponding to an H/L of 0.11. The surface of the debris avalanche is characterized by a pronounced hummocky morphology and steep margins. There are 256 conical hummocks up to 185 m high, most of them consisting of individual megaclasts. The deposit is monolithologic and consists of debris avalanche blocks of dacitic lava. It is associated with a 3-m-thick blast deposit intimately mixed with the uppermost 1–2 m of the avalanche deposit and capped by a tephra layer. Charcoal fragments found in the tephra unit yielded a radiocarbon age of 9690 ± 89 yr BP, which can be assumed to be the age of the collapse and debris avalanche.

Based on stratigraphic evidence, Siebe et al. (1992) consider that Bezymianny-type activity caused the edifice collapse. The direction of the failure is probably related to the predominantly E–W tectonic trend of the area (Acambay Graben) (Fig. 4). The emplacement of the debris avalanche deposit was followed by explosive activity that formed pyroclastic surges and fall units which ended with the formation of a dacitic dome. Considering the morphology of the deposit and its stratigraphic characteristics, Siebe et al. (1992) suggest a sequence of initial disaggregation of a large block into elongate ridges, and final disruption into large blocks which then separated



into individual megaclasts, and then were eroded to form the present conical hummocks. The collapse of the edifice started as a rockslide but final emplacement involved fluid-like spreading over the irregular topography.

6. The Nevado de Toluca Volcano

The Nevado de Toluca Volcano (NT; Figs. 1 and 5, Table 1) is an andesitic to dacitic strato-volcano at which activity started 2.6 Myr ago (García-Palomo et al., 2002). After a first stage of effusive activity, during which andesitic and dacitic lava flows constructed the central edifice, two major sector collapses destroyed the southern flank of the volcano (Macías et al., 1997). During the last 37 000 years at least five dome collapses (at about 37 000, 32 000, 28 000, 26 000 and 15 000 yr BP) yielded huge block-and-ash flows surrounding the volcano, and four major plinian eruptions formed the Ochre Pumice fall (36 000 yr BP, García-Palomo et al., 2002), the Lower Toluca Pumice (24 000 yr BP), the White Pumice Flow (12 500 yr BP), and the Upper Toluca Pumice (10 500 yr BP) pumice fall deposits (Bloomfield and Valastro, 1974, 1977; Macías et al., 1997).

Macías et al. (1997) recognized two debris avalanche deposits extending E–SE from the volcano to a distance of 55 km during Pleistocene time. Subsequent study (Capra and Macías, 2000) revealed that the younger sector collapse produced deposits which reached 75 km from the edifice, covering an area of 220 km² with a total volume of 2.8 km³ (Fig. 5). Two deposits constitute the sequence: the Pilcaya (PDF) and the El Mogote (MDF) cohesive debris flow deposits.

The PDF deposit starts to crop out 20 km from the volcano and extends up to 55 km, covering an area of 100 km². Estimating a minimum height of drop of 3000 m, an $H/L = 0.054$ is obtained. It

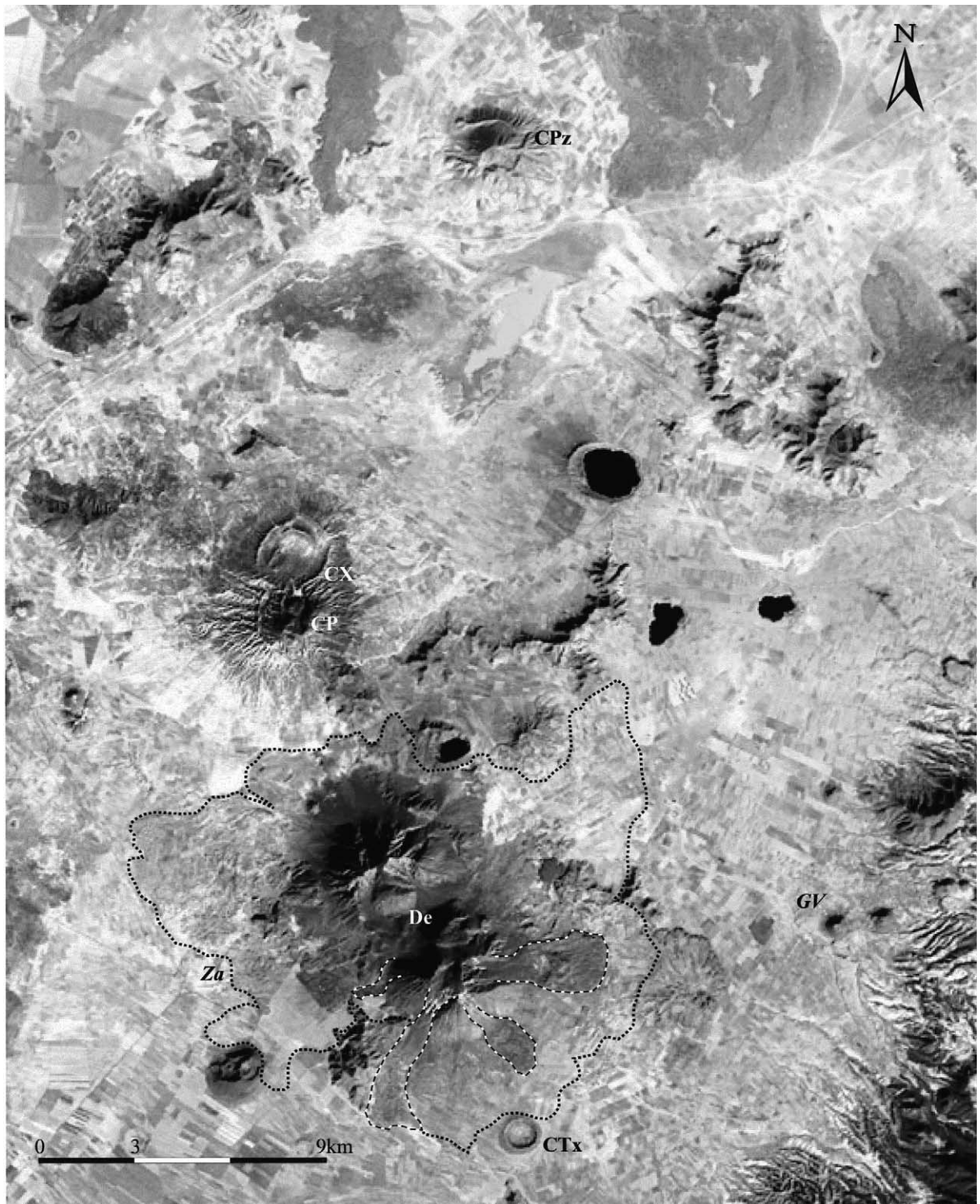
overlies the local basement and has a flat surface. Only in the medial area is hummocky morphology evident, with mounds up to 20 m high. The thickness of the PDF varies from 6 m in the proximal section to 40 m in the medial portion. Estimating an average thickness of 20 m yields a total volume of 2 km³.

The PDF unit consists of a massive, matrix-supported deposit containing megaclasts up to 15 m in diameter, some with jigsaw puzzle structure. It is heterolithic and contains clasts of andesite and dacite from the edifice and secondary fragments of rocks from the local basement, such as andesite and basalt of the Basal Sequence, limestone of the Balsas Formation, schist of the Ixtapán–Teloloapan Formation, rhyolite from the Tilzapotla Formation, and conglomerate and lacustrine fragments of the Tepoztlán Formation. The matrix is sandy (up to 80% sand), but contains up to 16% clay in the proximal areas. Sorting improves, and mean grain size decreases downstream.

The MDF deposit rests directly on top of the Pilcaya unit, cropping out at a distance of 40 km and extending up to 75 km from the edifice with an average thickness of 10 m and maximum thickness of 15 m. It covers an area of 120 km² with a total volume of 0.8 km³. It consists of a massive, matrix-supported deposit, contains clasts up to 1 m in diameter, and has the same composition of the Pilcaya deposit. The matrix is sandy (up to 78% sand) and contains up to 6% clay.

Based on the textural and sedimentological characteristics of the PDF, we infer that collapse of Nevado de Toluca volcano occurred due to the intense alteration (hydrothermal and weathering) and tectonic dissection of the edifice. A rapid change in topographic gradient in the medial zone (40 km from the volcano) provoked a decrease in the velocity of the flow, accompanied by abrupt thickening and deposition of large

Fig. 5. Landsat image of the central portion of the TMVB that shows, from left to right: Nevado de Toluca (NT), Sierra de Zempoala (Ze), Ajusco (Aj), Popocatepetl (Po), Iztaccíhuatl (Iz) and their relative debris avalanche/debris flow deposits (black-and-white dashed lines). The limit of the Ajusco debris avalanche deposit is uncertain because it is now buried by a thick volcanic sequence from the San Miguel dome complex (SM). Other volcanic centers are: Chichinautzin Volcanic Field (CVF) and Telapón (Te). Main cities are: Toluca (To), Cuernavaca (Cu), Mexico City (MC), and Puebla (Pu).



blocks preserved as hummocks. Capra and Macías (2000) speculate that, after some hours or days the upper part of the deposit mobilized to create the MDF.

7. Popocatepetl volcano

Popocatepetl volcano (Po, Figs. 1 and 5, Table 1) is a snow-capped andesitic composite cone. During the past 23 000 years activity has been characterized by at least seven large plinian eruptions producing pumice fall and ash flow deposits (Siebe et al., 1996). The last two eruptions occurred circa 2300 and 1200 yr BP. Although a horseshoe-shaped crater is not preserved, debris avalanche deposits were recognized by Robin and Boudal (1987), who reported a deposit probably less than 50 000 years old on the southern flank (Fig. 5), covering 300 km² with a volume of 28–30 km³. The *H/L* ratio is 0.116. Siebe et al. (1995b) recognized three distinct debris avalanche deposits that traveled at least 70 km south, much farther than the example reported by Robin and Boudal (1987). These deposits are very similar in extent, lithology and internal structure. They covered over 600 km² of the southern plain. Siebe et al. (1995b) assumed a height *H* of 4500 m for the cone prior to the collapse, obtaining an *H/L* of 0.064. Hummocks up to 300 m in height are present in the proximal area, but the southern distal plain is characterized by a flat surface. The deposits are heterolithologic, with clasts of andesite and dacite and fragments of older pyroclastic sequences. Both block and mixed facies are present, and the estimated average thickness is 15 m for each deposit, which yields a total volume of 27 km³.

Siebe et al. (1995b) concluded that the younger debris avalanche originated from Bezymianny-type activity, accompanied by a lateral blast, fol-

lowed by a plinian column yielding thick pumice and ash flow deposits. The ‘blast’ deposit is remarkable for its thickness, its distance from the source, and clast size (up to several meters in diameter more than 10 km from the source). The deposit consists mostly of sand, gravel, and boulders, with cross-stratification and an erosive basal contact. The age of the event is 22 875 ± 915 yr BP. The age of the older debris avalanche deposit is unknown.

More recently, Lozano-Velázquez and Carrasco-Núñez (1997) recognized a cohesive debris flow on the southern flank of the volcano, extending up to 45 km and covering an area of 200 km² with a volume of 0.5 km³. They infer that the flow originated on the medial slopes of the volcano and that its course was controlled by the distribution of the older debris avalanche deposits.

8. Las Derrumbadas dome complex

The Las Derrumbadas dome complex (De, Figs. 1 and 6, Table 1) is an example of debris avalanche generation during dome growth (Siebe et al., 1995a). The rhyolitic dome complex is located in the Serdan basin (Puebla State) and consists of two monogenetic dome structures (Fig. 6). Several debris avalanche deposits surround the domes to a distance of 9 km. Two types of deposits are recognized. The first-generation deposits were derived from 60–90° sector collapses. Deposits are heterolithologic and consist of a chaotic mixture of juvenile obsidian, blocks of faulted pyroclastic and surge flow deposits, as well as blocks of non-volcanic rocks such as Cretaceous limestones and partly consolidated lake sediments in a whitish clayey matrix. They display a typical hummocky topography and have *H/L* ratios of 0.1 and maximum runout distances of 9 km (Siebe et al., 1995a). The second-generation deposits are

Fig. 6. Landsat image of the Las Derrumbadas rhyolitic dome complex and other volcanic centers. The black dotted line delimits the distribution of the first-generation debris avalanche deposits while the black-and-white dashed lines delimit the second-generation debris avalanche deposits (after Siebe et al., 1995a). Other volcanic centers: Cerro Xalapasco tuff cone (CX), Cerro Pinto dome (CP) and Cerro Pizarro (CPz) which presents a horseshoe-shaped crater opened to the west. Main towns are: Zacatepec (Za) and Guadalupe Victoria (GV).

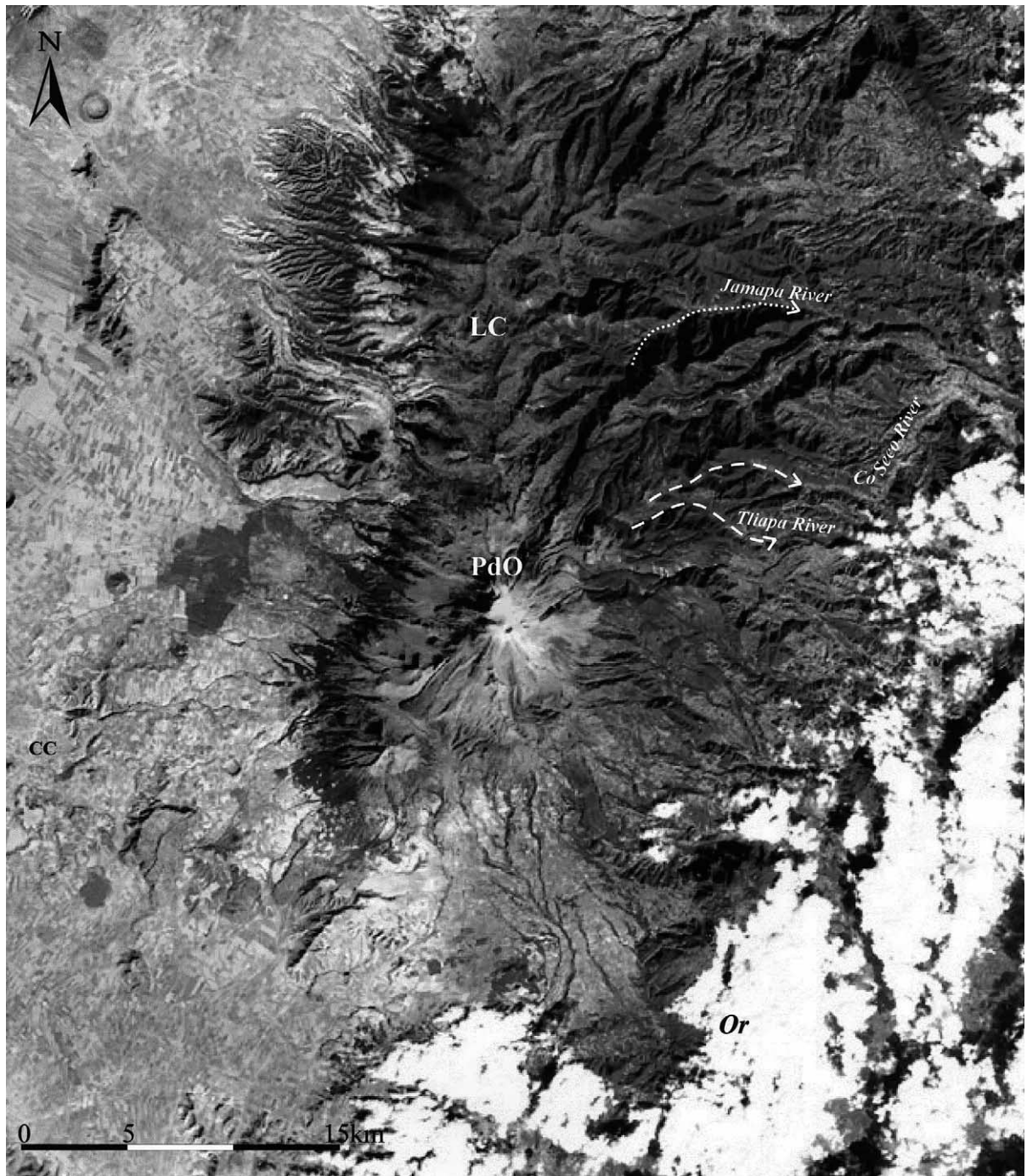


Fig. 7. Landsat image of the Pico de Orizaba volcano showing the flow trajectories on proximal zone for the Jamapa debris avalanche deposit (white dotted line) and the Tetelzingo lahar (white dashed line). Las Cumbres volcano (LC), north of Pico de Orizaba, shows a horseshoe-shaped crater associated with a debris avalanche deposit (see Table 1). Main cities are: Orizaba (Or), Coscomatepec (Co) and Ciudad Serdan (CC).

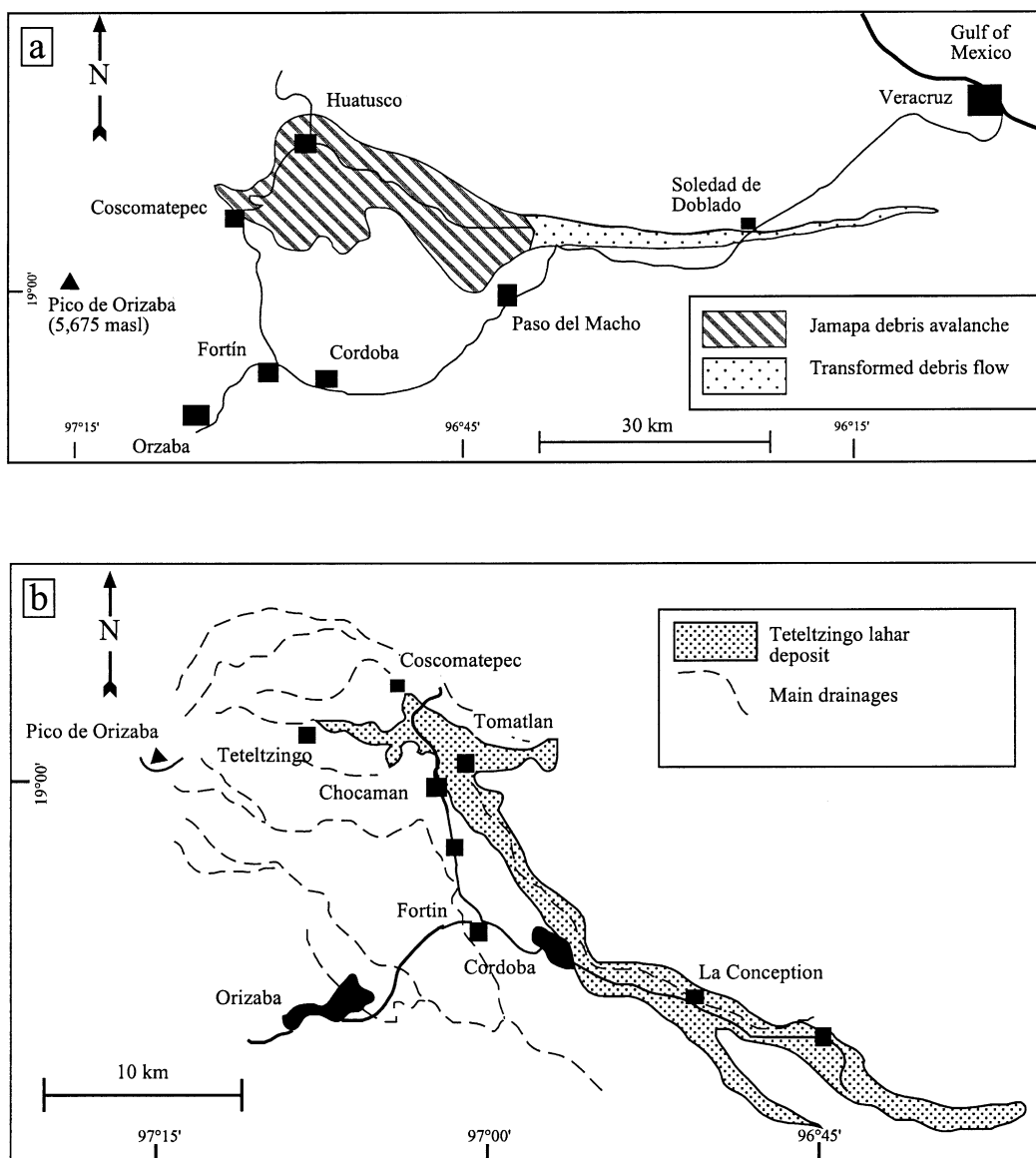


Fig. 8. Distribution of (a) the Jamapa debris avalanche deposit and (b) the Teteltzingo lahar at the Pico de Orizaba volcano (after Carrasco-Núñez et al., 1993; Carrasco-Núñez and Gómez-Tuena, 1997).

stratigraphically on top of the first-generation deposits, and originated from 20–30° sector collapses. They are monolithologic in composition, consist of gray microcrystalline rhyolite, and are finer-grained than the first-generation deposits. They form flat surfaces and have steep terminal scarps. They have a runout distance of 4.5 km

and an H/L ratio of 0.2. The first-generation debris avalanches originated during initial growth of the dome and the associated uplift of bedrock. The second-generation flows originated after dome formation from hydrothermally altered portions of the domes, marked by intense modern fumarolic activity.



9. Pico de Orizaba

Pico de Orizaba volcano (PdO, Figs. 1 and 7, Table 1) is an ice-capped, andesitic stratovolcano that at 5675 m asl is Mexico's highest peak (Fig. 7). The volcano has been active since the early Pleistocene, with its most recent activity dated at AD 1437–1687 (Simkin et al., 1981). The evolution of Pico de Orizaba during Pleistocene–Holocene times has been divided into three main stages (Carrasco-Núñez and Gomez-Tuena, 1997): (1) construction of the ancestral stratovolcano Torrecillas (Pleistocene); (2) construction of the superimposed cone Espolón de Oro (0.21 Ma); and (3) construction of the present cone (Early Holocene). Flank collapse has occurred between these major stages. Hoskuldsson and Robin (1993) described four separate debris avalanche deposits, one of which was interpreted as a block-and-ash flow deposit by Siebe et al. (1993), and two of them – the Jamapa avalanche and the Tetelzingo lahar – have been recognized to be related to collapses of the ancestral volcanoes on which the present cone has been built (Carrasco-Núñez et al., 1993; Carrasco-Núñez and Gomez-Tuena, 1997).

The Jamapa avalanche originated from a sector collapse of the Torrecillas cone during the Pleistocene (Figs. 7 and 8a). It extends eastward, up to a distance of 105 km, covering an area of 350 km² with a volume of approximately 20 km³. The deposit is massive, ungraded, heterolithologic, with boulders, gravel and cobbles in a silty-clay matrix. At a distance of about 75 km this unit changes laterally to a debris flow deposit. Considering the extension of the debris avalanche deposit a H/L of 0.05 is obtained.

The Tetelzingo lahar (Figs. 7 and 8b) originated from the flank failure of the Espolón de Oro cone between 27 000 and 13 000 yr BP. It also flowed toward the east from the volcano, reaching a distance of about 75 km, spreading over an area of 143 km² with a total volume of 1.8 km³. H/L is

0.055. It is worth mentioning here that the low H/L values obtained for these two deposits might reflect the impressive height difference of 4000 m between the Pico de Orizaba Volcano and the coastal plain.

The deposit represents a cohesive debris flow preserved as a single massive, poorly sorted mixture of heterolithologic pebbles, cobbles, and boulders in a characteristic yellow–brown sandy matrix with up to 16% clay fraction. It reached a maximum thickness of about 100 m in the proximal zone, with hummocky morphology extending in the medial zone to 30 km. Mounds are up to 15 m high (Carrasco-Núñez et al., 1993).

The authors attribute collapse to the instability of the edifice resulting from hydrothermal alteration and to glacial erosion that exposed more extensive areas of unstable, hydrothermally altered rock.

10. Other cases

Table 1 summarizes all the known cases of debris avalanche deposits from volcanoes of the TMVB, some of which are shown on the Geologic Map of Michoacán State (Garduño-Monroy et al., 1999).

10.1. Sierra de Zempoala

The Sierra de Zempoala (Ze, Figs. 1 and 5, Table 1) belongs to the N–S Las Cruces–Ajusco–Zempoala volcanic chain which separates the Mexico basin from the Toluca basin (Fig. 5). It is composed of a sequence of andesitic lava flows (Zempoala Andesite, Fries, 1960) with alternating volcanoclastic deposits in which clasts range in composition from andesite to rhyodacite. Its age ranges from Late Miocene to Pliocene (De Cserna et al., 1987). Fries (1960) has described a 200-m-thick volcanoclastic sequence (Cuernavaca Formation) but no more information on collapse-related

Fig. 9. Landsat image of the Tancitaro volcano. Note the huge fan formed by a debris flow deposit which originated from the collapse of the eastern flank (white arrow shows the debris flow trajectory). Black dashed line indicates the southern limit of the deposit. Main town is Uruapan (Ur).

debris flow deposits has been given for this area. Our observations suggest that during the Pliocene the eastern flank of the Zempoala volcano collapsed creating a large debris flow (Fig. 5). It extends 80 km toward the south, over an area of approximately 400 km² with an average thickness of 10 m that yields a volume of 4 km³. The deposit is massive, matrix-supported, and is dominated by dacitic clasts. Secondary clasts are all eroded from the bedrock, which ranges in composition from limestone, chert, sandstone, fragments of conglomeratic and lacustrine deposits, and basaltic lavas (rocks that constituted the basement of the area, ranging in age from Cretaceous to

Miocene). The content of the secondary components laterally change in abundance according to the exposure of the bedrock. The areal distribution of the deposit suggests that the paleotopography determined the emplacement behavior of the debris flow as it filled depressions to a maximum thickness of 40 m between limestone hills, on top of which are deposited overbank-like layers (up to 2 m thick).

10.2. Tancítaro volcano

The Tancítaro volcano (Ta, Figs. 1 and 9, Table 1) is an andesitic to dacitic composite cone

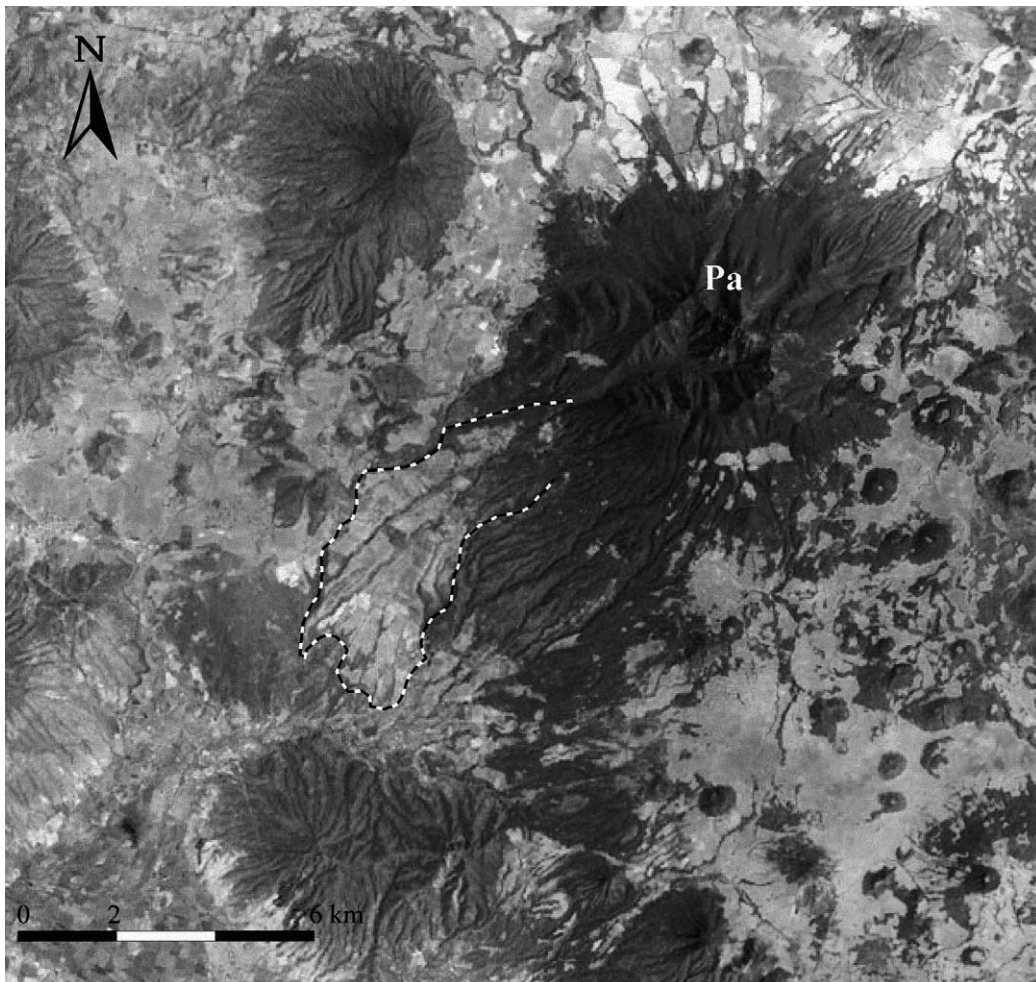


Fig. 10. Landsat image of the Patambán volcano showing the distribution of the debris avalanche deposit (black-and-white dashed line) emplaced towards the southwest.

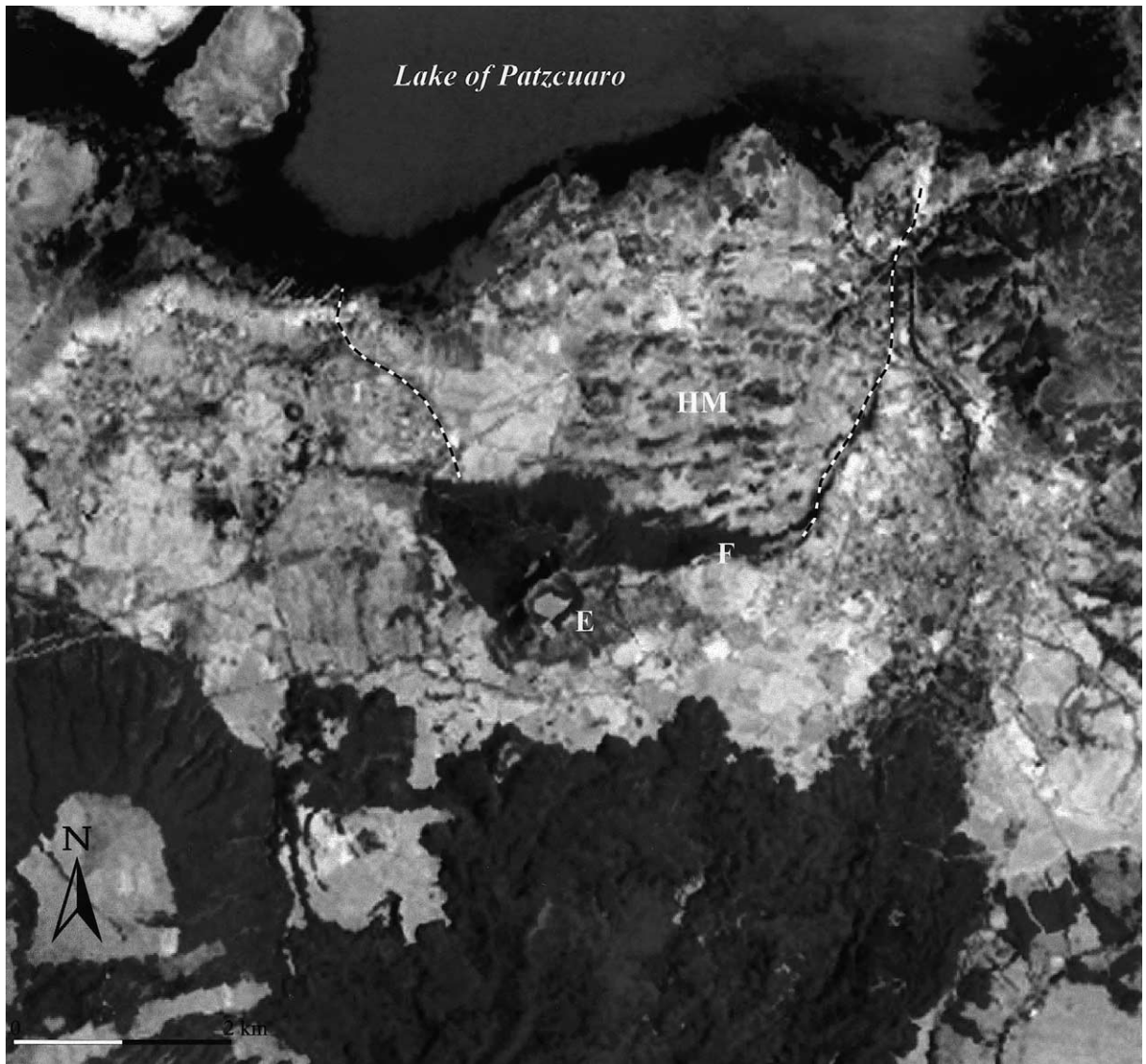


Fig. 11. Landsat image of the El Estribo cone and the limit of its debris avalanche deposit (black-and-white dashed line). Note the morphological expression of the E–W fault (F) responsible for the collapse, and the hummocky morphology (HM) which characterizes the deposit.

that is the most spectacular volcanic edifice in Michoacán State. It is located at the intersection of two tectonic structures, the NW–SE Chapala–Oaxaca fault system and the NE–SW fault system that characterizes the TMVB (Suter et al., 1992). Its morphology is characterized by U-shaped, glacially incised valleys on the northern flank (Garduño-Monroy et al., 1999), which are cut by an

east-facing horseshoe-shaped crater up to 4 km wide and containing a resurgent dome (Fig. 9). A debris flow deposit is directly associated with this structure and extends 60 km toward the southeast, covering an area of approximately 176 km² with an average thickness of 20 m, which yields a volume of 3.5 km³. It is massive, with dacitic and andesitic clasts embedded in a silty–



clay matrix. Based on the morphological relations between the crater and the glacial valleys, the collapse event is probably younger than 10 000 yr BP (Garduño-Monroy et al., 1999).

10.3. Patámban volcano

The Patámban volcano (Pa, Figs. 1 and 10, Table 1) is an andesitic composite cone with a 2-km-wide horseshoe-shaped crater open to the southwest (Fig. 10). This structure is associated with a debris avalanche deposit that extends for 9 km, covering an area of approximately 25 km² with an average thickness of 10 m (Table 1). The deposit is clast-supported and shows pervasive hydrothermal alteration. This deposit is directly associated with a plinian fall unit which probably represents the activity that followed the collapse (Garduño-Monroy et al., 1999). The age of this event is unknown.

10.4. El Estribo cone

El Estribo cone (Es, Figs. 1 and 11, Table 1) is an andesitic monogenetic cone associated with the volcanic field of the Corredor Tarasco, in Michoacán State. On its northern flank it has been influenced by a E–W normal fault which caused its partial collapse, forming a scarp extending 100 m above the level of the adjacent Lake of Patzcuaro (Fig. 11). The debris avalanche deposit extends 3 km along the shore of the lake and continues below the surface. The deposit has well-defined hummocky morphology, with elongated mounds in the flow direction as much as 40 m high and forming small islands in the lake (Huecorio, Uranden and Tzentzenguaro Islands). The hummocks are composed of andesite with typical jigsaw puzzle texture, separated by a small proportion of a sandy matrix. Lacustrine layers found at the base of the deposit yielded an age of 45 000 yr BP (Bradbury, 1998).

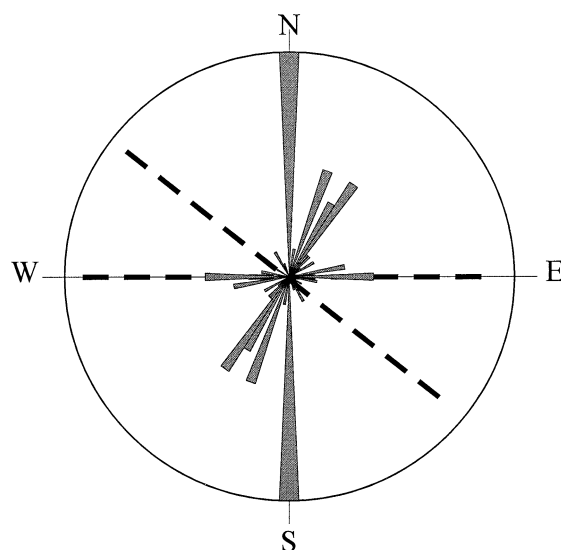


Fig. 13. Rose diagram for directions of the Mexican collapses in this study. The dashed lines represent the main tectonic stress directions on the TMVB, which are perpendicular to the main collapse directions.

10.5. Santa Martha volcanic field and San Martin Pajapan

The Santa Martha volcanic field and San Martin Pajapan volcano belong to the so-called ‘Los Tuxtles Volcanic Field’, a sodium-rich alkaline volcanic field located in eastern Mexico and isolated from the TMVB (Fig. 1). Nevertheless, these two volcanoes are described here because of spectacular morphological features that are directly related to debris avalanche deposits.

The Pliocene Santa Martha volcanic complex is located in Veracruz State (StM, Figs. 1 and 12, Table 1), southwest of the Tuxtles alkaline volcanic field, which contains more than 250 monogenetic cones. In contrast to the alkaline composition of the Los Tuxtles volcanic field, the Santa Martha complex ranges in composition from alkaline basalt to calc-alkaline basaltic andesite (Nelson and Gonzalez-Caver, 1992). Two horse-

Fig. 12. Landsat image of the Santa Martha Volcanic Complex (StM) that exhibits the two main horseshoe-shaped craters facing E–NE and the fans formed by their respective debris avalanche deposits (DA). Note the San Martin Pajapan volcano (SMP) that has a crater open to the southeast.

shoe-shaped craters, each 3.5 km in diameter, characterize the complex. The associated debris avalanche deposits extend for 20 km into the Gulf of Mexico (Fig. 12).

The San Martin Pajapan volcano (SPM, Figs. 1 and 12, Table 1) is located southwest of the Santa Martha complex. It is a Pliocene composite cone composed of calc-alkaline basaltic andesite rocks (Nelson and Gonzalez-Caver, 1992). Two craters open to the south are associated with debris avalanche deposits (Fig. 12).

The directions of the collapses at both the Santa Martha and San Martin Pajapan volcanoes are parallel to a NE–SW axis that possibly represents a paleodirection of tectonic stress that differs from the present tectonic regime of the TMVB.

11. Tectonic implications

Structural factors may predispose volcanoes to fail in a particular direction. From the studied cases within the TMVB, it is evident that the preferred directions of failure were southwards and northeastwards. Fig. 13 is a rose diagram with all the Mexican case histories, showing that the preferred directions of collapse are N–S and NE–SW. Some deviations from those principal trends, mainly in the E–W direction, are probably due to the local tectonic setting. This phenomenon can be explained by considering the main tectonic structures that characterize the TMVB. According to previous studies (Demant, 1978; Suter et al., 1992) the TMVB is mainly affected by two principal normal fault systems oriented E–W and NW–SE respectively. This implies that N–S and NE–SW are the directions of maximum distention (σ_3 vector). As observed in other volcanoes of the world (Siebert, 1984) the σ_3 direction corresponds with the main dispersal axis of debris avalanche deposits. The Nevado de Toluca volcano is affected by the E–W active Tenango normal fault (García-Palomo et al., 2000), with a N–S direction of distention that corresponds to the direction of the collapse described by Capra and Macías (2000). Popocatepetl volcano, with a southern flank that has suffered at least three collapses (Siebe et al., 1995b), is affected by the La Pera

E–W normal fault (Delgado et al., 1997) that according to these authors has a southwards extensive component. The Jocotitlán volcano is located 10 km south of the E–W Acambay Graben, and the main collapse direction corresponds with the direction of σ_3 (Siebe et al., 1992). The Colima Volcanic Complex is intersected by the normal Tamazula fault system (Garduño-Monroy et al., 1998), oriented SW–NE and possibly responsible for the trends of the main collapses of the Volcán de Colima and Nevado de Colima volcanoes (mainly toward the south and southeast).

The Pico de Orizaba, Las Cumbres and Cofre de Perote volcanoes, which form a N–S chain, are probably located on the trend of the N–NW normal Oaxaca fault (Nieto-Samaniego et al., 1995; Alaniz-Alvarez et al., 1996). Collapses of those edifices are all directed east or northeast.

We note that collapse may reflect the local stress field as well as the regional tectonic framework (Siebert, 1984).

12. Debris avalanche vs. debris flow: mobility and hazard assessment

Edifice collapse has occurred from a variety of volcanic structures in the TMVB – stratovolcanoes (e.g. Nevado de Toluca), composite cones (e.g. Popocatepetl, Colima and Pico de Orizaba), compound cones (e.g. Iztaccihuatl) and dome complexes (e.g. Las Derrumbadas). The sector collapses mainly were related to magma intrusion (e.g. Popocatepetl, Jocotitlán and Colima volcanoes) and generated debris avalanche deposits. Smaller flank collapses, mainly reflecting hydrothermal alteration of the edifice, are less certainly associated with magmatic activity and were more likely to yield cohesive debris flows (e.g. Pico de Orizaba and Nevado de Toluca) than the larger failures. In both cases the directions of collapses were strongly related to the regional tectonic stress field.

From the TMVB examples, it appears that debris avalanche deposits originate from magmatically triggered sector collapse, and that cohesive debris flows are more commonly associated with smaller flank failures. However, at other volca-

noes, debris avalanches and their characteristically mounded deposits may form from both sector and flank collapses. For example, at Mt. Rainier, a debris avalanche with mounded deposits occurred from a small flank collapse in 1963 (Crandell and Fahnestock, 1965; Scott et al., 1995). Also, cohesive debris flows can be the product of a direct transformation from a debris avalanche, or can result from post-depositional remobilization of a debris avalanche deposit, as in the case of the North Fork Toutle River lahar, which formed from the 1980 Mt. St. Helens debris avalanche deposit about 5 h after emplacement (Janda et al., 1981). Cohesive debris flows may also originate from rupture of a natural dam, as occurred with emplacement of the 18 500 yr BP debris avalanche deposit at Nevado de Colima volcano. From the above Mexican case histories the predisposition of a sliding mass to transform directly to a cohesive debris flow is strongly dependent on conditions prior to failure such as water content and hydrothermal alteration. Such conditions are common in the large, ice-capped stratovolcanoes of the TMVB.

The mobility of both debris avalanches and debris flows produced from volcano collapse is critical to evaluating the areas at risk from future events. Factors that control runout distance of

flows commonly described as debris avalanches are the fall height (Hsu, 1975), the volume of the sliding mass (Siebert, 1984), and its coefficient of friction (Dade and Huppert, 1998). The Heim parameter H/L represents the coefficient of friction of a landslide mass (Hsu, 1975) and a debris avalanche (Siebert, 1984). The drop height H is the difference in vertical elevation of the debris avalanche source and its final position; the runout distance L is the horizontal distance from source to terminus. The H/L ratio defines a line representing the energy transformation (potential-kinetic) of an avalanche mass during flow. It has been used to describe the mobility, to estimate the velocity, and to predict flow paths in debris avalanche hazard assessment (Siebert et al., 1987; Crandell, 1989; Schuster and Crandell, 1984).

Many volcanic debris flows originate by collapse of hydrothermally altered parts of an edifice. The failed mass transforms directly into a cohesive (> 3% in clay fraction) debris flow, with mobility that can be attributed to the presence of abundant clay-size material in the matrix and to a high water content. Grain interactions are cushioned by clay aggregates that adhere to larger particles and reduce near-boundary interaction between clasts. In addition, the clayey matrix retards the settling of coarse-phase particles and

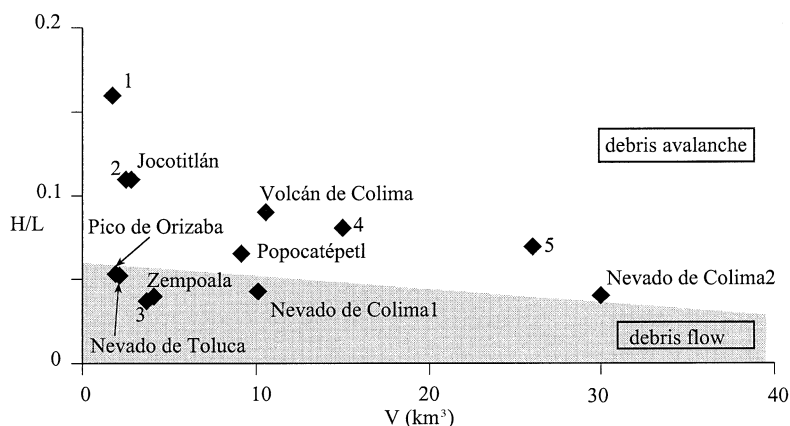


Fig. 14. Diagram of H/L vs. V (volume) for the Mexican cases in this study and some examples of cohesive debris flows (3: Osceola Mudflow, Mt. Rainier, Vallance and Scott, 1997) and volcanic debris avalanche deposits of the world (from Siebert et al., 1987). 1: Bezymianny. 2: Mt. St. Helens. 4: Socompa. 5: Shasta. The Nevado de Colima data is plotted twice: (1) based on the model proposed by Stoopes and Sheridan (1992), and (2) based on the interpretation proposed by Capra and Macías (1999, 2002).

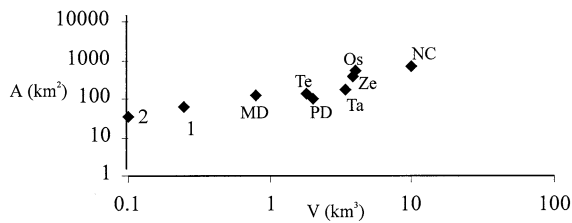


Fig. 15. A/V diagram for the studied debris flow deposits and other known cases. Abbreviations are: Mogote deposit (MD), Pilcaya deposit (PD), both from the Nevado de Toluca (Capra and Macías, 2000); Tetelzingo lahar (Te), Pico de Orizaba (Carrasco-Núñez et al., 1993); Tancitaro debris flow (Ta) (this work); Zempoala debris flow deposit (Ze) (this work). The Colima value is plotted based on the interpretation proposed by Capra and Macías (2002). Other known cases: Electron Mudflow (1), Paradise lahar (2) and Osceola mudflow (3), Mt. Rainier (Crandell, 1971; Vallance and Scott, 1997).

their differential movement, promoting and facilitating the transport of the mass over great distances with respect to other types of flows (e.g. granular or noncohesive debris flows) (Scott et al., 1995). It is also important to note that the volumes of these flows may enlarge during flow (bulking) by incorporating additional sediment eroded from the flow boundary. Bulking observed in the examples reported here is as much as six times in the case of Nevado de Colima (Capra and Macías, 2002).

Debris flows normally fill depressions, and may attain their maximum thickness some distance from the edifice, where valleys widen and gradients become lower, as observed at Nevado de Toluca volcano (Capra and Macías, 2000). During peak flow, debris flows may leave overbank deposits, as observed in the case of the Tetelzingo lahar deposit at the Pico de Orizaba (Carrasco-Núñez et al., 1993).

Debris flow behavior is related to many different variables and would be substantially underestimated by use of the H/L parameter. Debris flows are far more mobile with respect to debris avalanches. H/L values calculated for the debris flows described here (0.03–0.05) are very low compared to the average values for debris avalanches (0.13–0.09). In particular, debris flows from Nevado de Toluca, Pico de Orizaba and

Nevado de Colima represent the most mobile flows, and their H/L ratios are approximately 0.04 (Fig. 14).

Vallance and Scott (1997) and Iverson et al. (1998) proposed that the relation of inundation area vs. flow volume is a better indication of flow mobility than runout distance vs. flow volume. In a plot of this parameter for cohesive debris flows, the deposit of the Nevado de Colima volcano is the most mobile event (Fig. 15). Iverson et al. (1998) proposed a model to delineate hazard zonation for debris flows in which they established that the area covered by a flow is proportional to its volume by the relation of $A = 0.05 V^{2/3}$. By knowing the volumes of previous debris flows, it is possible to delineate the potential future inundation area around a volcano. It is important to note that the topography of the inundated area is crucial to the behavior of both debris flows and debris avalanches. As observed at Nevado de Colima volcano (Capra and Macías, 1999), the debris avalanche stopped against a topographic barrier, forming a temporary dam, the failure of which produced a huge cohesive debris flow. This fact indicates that particular topographic conditions around a volcano can be responsible for a secondary flow that can affect a far larger area than was inundated by the primary flow. This phenomenon is relatively common and has been observed in cases such as the 1980 Mt. St. Helens eruption, where the debris avalanche deposit formed at least three different dams that did not fail only because they were drained by engineering works (Costa, 1984).

13. Conclusions

Stratovolcanoes of the TMVB have yielded up to three collapse events at each center, as in the case of Popocatepetl volcano. In particular, Popocatepetl, Jocotitlán and Volcán de Colima volcanoes could collapse in the future at the time of renewed magmatic activity. Popocatepetl and Colima volcanoes are now characterized by dome formation (Smithsonian Institution's Global Volcanism, 1996, 1999), and the probability of a flank collapse is increased, especially considering their

steep flanks, sloping between 35° and 40°. Nevado de Toluca and Pico de Orizaba volcanoes are at lower risk of collapse because of their present inactivity. Pico de Orizaba, however, has a large ice cap and a pervasive zone of hydrothermal activity (Hubbard et al., 1999) and has potential to fail from such causes as increase in pore water pressure from heavy rains and hurricanes, phreatic explosions, and earthquakes. In particular, the 1998 sector collapse of the Casita volcano (Nicaragua) demonstrates that abnormal and prolonged rainfall can induce the failure of a hydrothermally altered portion of an edifice, without any precursory signs.

The products of volcano collapse are classified as debris avalanche and debris flow deposits, depending on their origin, texture, and sedimentological characteristics. Based on runout distance and inundation areas, debris flows are more mobile than debris avalanches. The *H/L* ratio remains the basic parameter delineating the areas at risk from debris avalanches. This method has been correctly used in the case of Popocatepetl, Colima, and Tres Virgenes volcanoes (Macías et al., 1995; Del Pozzo et al., 1996; Capra et al., 1998). In the case of volcanic edifices where factors such as an ice cap, hydrothermal alteration, water saturation, and strong regional tectonic stress could promote flank failure, as has been the case with Nevado de Toluca and Pico de Orizaba volcanoes, the relation of *V/A* better describes the potential flow behavior. This parameter is most useful when combined with analysis of the pre-existing topography. We suggest particular caution for hazard zonation of debris flows, with special attention to changes in topographic gradient and transitions from channeled to flat areas that could significantly affect the inundated area. We also suggest consideration be given to the possibility of blockages of river valleys by debris avalanches and consequent formation of debris flows when the avalanche deposit fails or is overtopped. Finally, we note that both debris avalanches and debris flows are volcanic hazards that occur from both active volcanoes, as well as those that are inactive or dormant volcanoes, and may be triggered by earthquakes, precipitation, or

simply gravity. There will be no precursory warning in such cases.

Acknowledgements

This work was supported by Grants CONACYT 27993-T to J.L.M., and IN100999 to J.L.M. and L.C. V. Neall and A. Borgia provided useful comments and ideas to the manuscript.

References

- Alaniz-Alvarez, S.A., van der Heyden, Nieto-Samaniego, A.F., Ortega-Gutierrez, F., 1996. Radiometric and kinematic evidence for Middle Jurassic strike-slip faulting in southern Mexico related to the opening of the Gulf of Mexico. *Geology* 24, 113–116.
- Avila, G.E., Caro, P.E., Cepeda, H., Moreno, M., Torres, P., and Agudelo, A., 1995. Zonificación para uso del suelo en la cuenca del Río Paez. *Jornadas Geotectónicas, VIII, Sociedad Colombiana de Ingenieros y Sociedad Colombiana de Geotecnia*, no. 6.79–6.102.
- Bloomfield, K., Valastro, S., 1974. Late Pleistocene eruptive history of Nevado de Toluca Volcano, central Mexico. *Bull. Volcanol.* 85, 901–906.
- Bloomfield, K., and Valastro, S., 1977. Late Quaternary tephrochronology of Nevado de Toluca volcano, central Mexico. *Overseas Geology and Mineral Resources* 46, 15 pp.
- Borgia, A., Ferrari, L., Pasquaré, G., 1992. Importance of gravitational spreading in the tectonic and volcanic evolution of Mount Etna. *Nature* 357, 231–235.
- Bradbury, P., 1998. A paleolimnological record of climate from Lago de Patzcuaro for the past 45 Ky. In: *Biennial Meeting of the American Quaternary Association, Puerto Vallarta*, p. 91.
- Capra, L., Macías, J.L., Espindola, J.M., Siebe, C., 1998. Holocene plinian eruption of La Virgen volcano, Baja California, Mexico. *J. Volcanol. Geotherm. Res.* 80, 239–266.
- Capra, L., Macías, J.L., 1999. Failure of a natural dam: the 27 km³ Cohesive Debris Flow originated from the Pleistocene debris avalanche deposit of Nevado de Colima volcano (Mexico). *EOS Trans. AGU*, F1173.
- Capra, L., Macías, J.L., 2000. Pleistocene cohesive debris flows at Nevado de Toluca Volcano, central Mexico. *J. Volcanol. Geotherm. Res.* 102, 149–168.
- Capra, L., Macías, J.L., 2002. Failure of a natural dam: the 10 km³ cohesive debris flow originated from the Pleistocene debris avalanche deposit of Nevado de Colima Volcano (Mexico). In: *Volcán de Colima, México, and its activity in 1997–2000*. *J. Volcanol. Geotherm. Res.* (in press).
- Carrasco-Núñez, G., Vallance, J.W., Rose, W.I., 1993. A voluminous avalanche-induced lahar from Citlaltepétl volcano,

- Mexico: Implications for hazard assessment. *J. Volcanol. Geotherm. Res.* 59, 35–46.
- Carrasco-Núñez, G., Gomez-Tuena, A., Volcanogenic sedimentation around Citlaltépetl volcano (Pico de Orizaba) and surroundings, Veracruz., Mexico. In: Aguirre-Diaz, G.J., Aranda-Gomez, J.J., Carrasco-Núñez, G., Ferrari, L. (Eds.), *Magmatism and Tectonics in the Central and Northwestern Mexico – A Selection of the 1997 IAVCEI General Assembly Excursions*. UNAM, Instituto de Geología, Mexico, D.F., pp. 131–151.
- Cervantes, P., Delgado, H., Molinero, R., 1994. Southern Mexico City settled on a debris avalanche deposit and basaltic lava flows: Late Pleistocene-Holocene volcanic history. *EOS Trans. AGU* 75, 737.
- Costa, J.E., 1984. The physical geomorphology of debris flow. In: Costa, J.E., Fleisher, P.J. (Eds.), *Developments and Applications of Geomorphology*. Springer-Verlag, Berlin, pp. 268–317.
- Costa, J.E., 1988. Floods from dam failures. In: Baker, V.R., Kochel, R.C., Patton, P.C. (Eds.), *Flood Geomorphology*. Wiley and Sons, New York, pp. 439–463.
- Costa, J.E., Shuster, R.L., 1988. The formation and failure of natural dams. *Geol. Soc. Am. Bull.* 100, 1054–1068.
- Crandell, D.R., 1971. Postglacial lahars from Mount Rainier volcano, Washington. *U.S. Geol. Surv. Prof. Pap.* 677, 75 pp.
- Crandell, D.R., 1989. Gigantic debris avalanche of Pleistocene age from ancestral Mount Shasta volcano, California, and debris avalanche zonation. *U.S. Geol. Surv. Bull.* 1861, 32 pp.
- Crandell, D.R., Fahnestock, R.K., 1965. Rockfalls and avalanches from Little Tahoma Peak on Mount Rainier, Washington. *U.S. Geol. Surv. Bull.* 1221-A, 30 pp.
- Crowley, J.K., Zimbelman, D.R., 1997. Mapping hydrothermally altered rocks on Mount Rainier, Washington, with Airbone Visible/Infrared Imaging Spectrometer (AVIRIS) data. *Geology* 25, 559–562.
- Dade, W.B., Huppert, H.E., 1998. Long-runout rockfall. *Geology* 26, 769–864.
- Day, S.J., 1996. Hydrothermal pore fluid pressure and the stability of porous, permeable volcanoes. In: McGuire, W.J., Jones, A.P., Neuberg, J. (Eds.), *Volcano Instability on the Earth and Other Planets*, *Geol. Soc. Spec. Publ.*, pp. 77–93.
- De Cserna, Z., de la Fuente-Duch, M., Palacio-Neto, M., Triay, L., Mitre-Salazar, L.M., Mota-Palomino, R., 1987. Estructura geológica, gravimétrica y relaciones neotectónicas regionales de la Cuenca de México. *Bol. Inst. Geol. UNAM.*, México 104, 71.
- Delgado, H., Nieto-Obregon, J., Lermo-Samaniego, J., Silva-Romo, G., Mendoza-Rosales, C., Campos-Enriquez, O., 1997. La Pera fault system: A major active structure in central Mexico. *EOS Trans. AGU* 78, 823.
- Del Pozzo, A.L., Sheridan, M.F., Barrera, D., Hubp, J.L., Vázquez, L., 1996. Mapa de peligros Volcán de Colima. Instituto de Geofísica, UNAM.
- Demant, A., 1978. Características del Eje Neovolcánico Transmexicano y sus Problemas de Interpretación. *Rev. Inst. Geol. UNAM México* 2, 172–186.
- Dzurisin, D., 1998. Geodetic detection of inflating stratovolcanoes: a potential breakthrough for mitigating volcanic hazards in the 21st century. *EOS Trans. AGU* 79, 973.
- Elsworth, D., Voight, B., 1996. Dike intrusion as a trigger for large earthquakes and the failure of volcano flanks. *J. Geophys. Res.* 100, 6005–6024.
- Francis, P.W., Wells, G.L., 1988. Landsat thematic mapper observation of debris avalanche deposits in Central Andes. *Bull. Volcanol.* 50, 258–278.
- Frank, D., 1983. Origin, distribution and rapid removal of hydrothermally formed clay at Mount Baker, Washington. *U.S. Geol. Surv. Prof. Pap.* 1022-E, 31.
- Fries, C., 1960. Geología del Estado de Morelos y de partes adyacentes de México y Guerrero. Región central meridional de México. *Bol. Inst. Geol. UNAM México*, 60, 234.
- García-Palomo, A., Macías, J.L., Garduño-Monroy, V.H., 2000. Miocene to Recent structural evolution of the Nevado de Toluca volcano region, Central Mexico. *Tectonophysics* 318, 281–302.
- García-Palomo, A., Macías, J.L., Arce, J.L., Capra, L., Espíndola, J.M., Garduño-Monroy, V.H., 2002. Geology of Nevado de Toluca Volcano and surrounding areas, central Mexico. *Map and Chart Series MCH099*, 14pp.
- Garduño-Monroy, V.H., Saucedo, R., Jimenez, S., Gavilanes, J.C., Cortes, A., Uribe, R.M., 1998. La Falla Tamazula, límite suroccidental del bloque Jalisco, y sus relaciones con el complejo volcánico de Colima, México. *Rev. Mex. Ci. Geol.* 15, 132–144.
- Garduño-Monroy, V.H., Corona-Chavéz, P., Israde-Alcantara, I., Mennella, L., Arreygüe, E., Bigioggero, B., Chiesa, S., 1999. Carta Geológica de Michoacán, scale 1:250,000. Universidad Michoacana de San Nicolás de Hidalgo.
- Glicken, H., 1991. Sedimentary architecture of large volcanic-debris avalanches. In: Smith, G.A., Fisher, R.V. (Eds.), *Sedimentation in Volcanic Settings*. *SEPM, Spec. Publ.* 45, pp. 99–106.
- Glicken, H., 1998. Rockslide-debris avalanche of May 18, 1980, Mount St. Helens Volcano, Washington. *Bull. Geol. Surv. Japan* 49, 55–106.
- Gorshkov, G.S., 1962. On the classification and terminology of Pelée and Katmai type eruption. *Bull. Volcanol.* 24, 155–165.
- Hoskuldsson, A., Robin, C., 1993. Late Pleistocene to Holocene eruptive activity of Pico de Orizaba, Eastern Mexico. *Bull. Volcanol.* 55, 571–587.
- Hsu, K.J., 1975. Catastrophic debris stream (Sturzstroms) generated by rockfalls. *Geol. Soc. Am. Bull.* 86, 129–140.
- Hubbard, B.E., Zimbelman, D.R., Crowley, J.K., Sheridan, M.F., Carrasco-Núñez, G., 1999. A comparison of two spectral analysis methods for identifying and Mapping hydrothermal alteration zone. *EOS Trans. AGU*, F1173.
- Janda, R.J., Scott, K.M., Nolan, K.M., Martinson, H.A., 1981. Lahar movement, effects and deposits. In: Lipman, P., Mullineaux, D.R. (Eds.), *The 1980 Eruptions of Mount*

- St. Helens, Washington. U.S. Geol. Surv. Prof. Pap. 1250, pp. 461–478.
- Keefer, D.K., 1984. Landslides caused by earthquakes. *Geol. Soc. Am. Bull.* 95, 406–421.
- Komorowski, J.C., Navarro, C., Cortes, A., Siebe, C., 1994. The repetitive collapsing nature of Colima volcanoes (Mexico). In: Problems related to the distinction of multiple deposits and the interpretation of ^{14}C ages with implications for future hazards. Colima Volcano Fourth International Meeting, Mexico, pp. 12–18.
- Komorowski, J.C., Navarro, C., Cortes, A., Saucedo, R., Gavilanes, J.C., Siebe, C., Espíndola, J.M., Rodríguez-Elizarrarás, S.R., 1997. The Colima Volcanic Complex. Field guide 3. In: IAVCEI, General Assembly, Puerto Vallarta.
- INGEOMINAS, 1995. El sismo del 6 de junio de 1994. I Seminario de Sismotectónica de Colombia. Memorias, Bogotá, 5 pp.
- Iverson, R.M., 1997. The physics of debris flows. *Rev. Geophys.* 35, 245–296.
- Iverson, R.M., Schilling, S.P., Vallance, J.W., 1998. Objective delineation of lahar-inundation hazard zones. *Geol. Soc. Am. Bull.* 110, 972–984.
- Lozano-Velazquez, L., Carrasco-Núñez, G., 1997. Laharic sequences at the southwestern flank of Popocatepetl volcano, Mexico. IAVCEI General Assembly, Puerto Vallarta, Abstract, p. 95.
- Lozano-Velazquez, L., Carrasco-Núñez, G., Evidencias del colapso sectorial del Volcán Cofre de Perote. 7ª Reunión Internacional Volcán de Colima, Abstract, p. 66.
- Luhr, J.F., Prestegard, K.L., 1988. Caldera formation at Volcán de Colima, Mexico, by large Holocene volcanic debris avalanche. *J. Volcanol. Geotherm. Res.* 35, 335–348.
- Macías, J.L., Carrasco-Núñez, G., Delgado, H., Del Pozzo, A.L., Siebe, C., Hoblitt, R.P., Sheridan, M.F., Tilling, R.I., 1995. Mapa de peligros volcánicos del Popocatepetl. Instituto de Geofísica, UNAM.
- Macías, J.L., Garcia-Palomo, A., Arce, J.L., Siebe, C., Espíndola, J.M., Komorowski, J.C., Scott, K.M., 1997. Late Pleistocene-Holocene Cataclysmic Eruptions at Nevado de Toluca and Jocotitlán Volcanoes, Central Mexico. In: Link, P.K., Kowallis, B.J. (Ed.), Proterozoic to Recent Stratigraphy, Tectonics, and Volcanology, Utah, Nevada, Southern Idaho and Central Mexico. *BYU Geol. Stud. Park I*, pp. 493–528.
- McGuire, W.J., Jones, A.P., 1996. Volcano instability: a review of contemporary themes. In: McGuire, W.J., Jones, A.P., Neuger, J. (Eds.), *Volcano Instability on the Earth and Other Planets*. *Geol. Soc. Spec. Publ.* 100, pp. 25–43.
- Moriya, I. 1980. Bandaian Eruption and landforms associated with it. Collection of articles in memory of retirement of Prof. K. Nishimura from Tohoku University, pp. 214–219.
- Nelson, S.A., Gonzalez-Caver, E., 1992. Geology and K-Ar dating of the Tuxtla Volcanic Field, Veracruz, Mexico. *Bull. Volcanol.* 55, 85–96.
- Nelson, S.A., Lighthart, A., 1997. An ancient buried debris avalanche deposit from Sierra Las Navajas, Hidalgo, Mexico. IAVCEI General Assembly, Puerto Vallarta, Abstract, p. 158.
- Nieto-Samaniego, A.F., Alaniz-Alvarez, S.A., Ortega-Gutierrez, F., 1995. Estructura interna de la falla de Oaxaca (México) e influencia de las anisotropías litológicas durante su actividad cenozoica. *Rev. Mex. Ci. Geol.* 12, 1–8.
- Palmer, B.A., Neall, V.E., 1989. The Murimotu Formation—9500 year old deposits of a debris avalanche and associated lahars, Mount Ruapehu, North Island, New Zealand. *N.Z. J. Geol. Geophys.* 32, 477–486.
- Pierson, T.C., Costa, J.E., 1987. A rheologic classification of subaerial sediment-water flows. In: Costa, J.E., Wiczorek, G.F. (Eds.), *Debris Flows/Avalanches: Process, Recognition, and Mitigation*. *Geol. Soc. Am. Rev. Eng. Geol.*, pp. 1–12.
- Robin, C., Boudal, C., 1987. A gigantic Bezymianni-type event at the beginning of modern volcan Popocatepetl. *J. Volcanol. Geotherm. Res.* 31, 115–130.
- Robin, C., Mossand, P., Camus, G., Cantagrel, J.-M., Gourgaud, A., Vincent, P.M., 1987. Eruptive history of the Colima volcanic complex (Mexico). *J. Volcanol. Geotherm. Res.* 31, 99–113.
- Robin, C., Komorowski, J.C., Boudal, C., Mossand, P., 1990. Mixed-magma pyroclastic surge deposits associated with debris avalanche deposits at Colima volcanoes, Mexico. *Bull. Volcanol.* 52, 391–403.
- Rodríguez-Elizarrarás, S.R., Komorowski, J.C., 1997. Las Cumbres volcanic complex, eastern Trans-Mexican Volcanic Belt (TMVB) geological evolution and characteristics of the main pyroclastic deposits. 1997 IAVCEI General Assembly, Puerto Vallarta, Abstract, p. 154.
- Schuster, R.L., Crandell, D.R., 1984. Catastrophic debris avalanches from volcanoes. In: *IV International Symposium on Landslides Proceedings*, Vol. 1, pp. 567–572.
- Scott, K.M., Vallance, J.W., Pringle, P.T., 1995. Sedimentology, behavior and hazards of debris flows at Mount Rainier, Washington. U.S. Geol. Surv. Prof. Pap. 1547, 56 pp.
- Scott, K.M., Macías, J.L., Vallance, J.W., Naranjo, J.A., Rodríguez, S., McGeehin, J.P., 2001. Catastrophic debris flows transformed from landslides in volcanic terrains: mobility, hazard assessment, and mitigation strategies. U.S. Geol. Surv. Prof. Pap. 1630, 67 pp., 19 figs., 9 tabs.
- Scott, K.M., Kerle, N., Macías, J.L., Strauch, W., Devoli, G., 2002. Catastrophic, precipitation-triggered lahars at Casita Volcano, Nicaragua – Flow transformations, flow bulking, and future mitigation strategies. *GSA Bull.* (submitted).
- Sheridan, M.F., Bonnard, C., Carreno, C., Siebe, C., Strauch, W., Navarro, M., Calero, J.C., Trujillo, N.B., 1999. Report on the 30 October 1998 rock fall/avalanche and breakout flow of Casita Volcano, Nicaragua, triggered by Hurricane Mitch. *Landslide News* 12, 2–4.
- Schuster, R.L., Crandell, D.R., 1984. Catastrophic debris avalanches from volcanoes. In: *IV International Symposium on Landslides Proceedings*, pp. 567–572.
- Siebe, C., Komorowski, J.C., Sheridan, M.F., 1992. Morphology and emplacement collapse of an unusual debris ava-

- lanche deposit at Jocotitlán Volcano, Central Mexico. *Bull. Volcanol.* 54, 573–589.
- Siebe, C., Abrams, M., Sheridan, M.F., 1993. Holocene block-and-ash flow fan at the W slope of ice-capped Pico de Orizaba volcano, Mexico – implications for future hazards. *J. Volcanol. Geotherm. Res.* 59, 1–31.
- Siebe, C., Macías, J.L., Abrams, M., Rodríguez-Elizarrarás, S.R., Castro, R., Delgado, H., 1995a. Quaternary explosive volcanism and pyroclastic deposits in East Central Mexico: Implication for future hazards. *Geol. Soc. Am. Annu. Meet.* 1995, New Orleans, LA, Field Trip Guide Book no. 1, 47 pp.
- Siebe, C., Abrams, M., Macías, J.L., 1995b. Derrumbes gigantes, depósitos de avalancha de escombros y edad del actual cono del volcán Popocatepetl. In: *Volcán Popocatepetl, Estudios realizados durante la crisis del 1994–1995*. CEN-APRED (Centro Nacional de Prevención de Desastres), UNAM, México D.F., pp. 195–220.
- Siebe, C., Abrams, M., Macías, J.L., Obenholzner, J., 1996. Repeated volcanic disasters in Prehispanic time at Popocatepetl, central Mexico: Past key to the future? *Geology* 24, 399–402.
- Siebert, L., 1984. Large volcanic debris avalanches: characteristics of source areas, deposits and associated eruptions. *J. Volcanol. Geotherm. Res.* 22, 163–197.
- Siebert, L., Glicken, H., Ui, T., 1987. Volcanic hazards from Bezymianny- and Bandai-type eruptions. *Bull. Volcanol.* 49, 435–459.
- Simkin, T., Siebert, L., McClelland, L., Bridge, D., Newhall, C., Latter, J.H., 1981. *Volcanoes of the World. A Regional Directory, Gazetteer, and Chronology of Volcanism During the Last 10,000 Years*. Hutchinson and Ross, Stroudsburg, PA.
- Smith, G.A., Fritz, W.J., 1989. Volcanic influences on terrestrial sedimentation. *Geology* 17, 375–376.
- Smithsonian Institution's Global Volcanism, 1996. Summary of recent volcanic activity. *Bull. Volcanol.* 58, 246–247.
- Smithsonian Institution's Global Volcanism, 1999. Summary of recent volcanic activity. *Bull. Volcanol.* 61, 423–424.
- Stoopes, G.R., Sheridan, M.F., 1992. Giant debris avalanches from the Colima Volcanic Complex, Mexico: Implication for long-runout landslides (>100 km). *Geology* 20, 299–302.
- Suter, M., Quintero, O., Johnson, C.A., 1992. Active faults and state of stress in the central part of the Mexican Volcanic Belt: the Venta de Bravo fault. *J. Geophys. Res.* 97, 11983–11994.
- Ui, T., Yamamoto, H., Suzuki-Kamata, K., 1986. Characterization of debris avalanche deposits in Japan. *J. Volcanol. Geotherm. Res.* 29, 231–243.
- Vallance, J.W., 2000. Lahars. In: Sigurdsson, H. (Ed.), *Encyclopedia of Volcanoes*. Academic Press, San Diego, CA, pp. 601–616.
- Vallance, J.V., Siebert, L., Rose, W.I., Girón, J.R., Banks, N.G., 1995. Edifice collapse and related hazard in Guatemala. *J. Volcanol. Geotherm. Res.* 66, 337–355.
- Vallance, J.V., Scott, K.M., 1997. The Osceola Mudflow from Mount Rainier: Sedimentological and hazard implication of a huge clay-rich debris flow. *Geol. Soc. Am. Bull.* 109, 143–163.
- van Wyk de Vries, B., Borgia, A., 1996. The role of basement in volcano deformation. In: McGuire, M.J., Jones, A.P., Neuberg, J. (Eds.), *Volcano Instability on the Earth and Other Planets*. *Geol. Soc. Spec. Publ.* 110, pp. 95–110.